

UNIVERSITÀ DEGLI STUDI DI SALERNO

DIPARTIMENTO DI MEDICINA, CHIRURGIA ED ODONTOIATRIA



CORSO DI DOTTORATO IN

**MEDICINA TRASLAZIONALE DELLO SVILUPPO E
DELL'INVECCHIAMENTO ATTIVO
XXXIV CICLO**

***CIRCULATING SORTILIN LEVEL AS A POTENTIAL BIOMARKER FOR
ENDOTHELIAL DYSFUNCTION AND HYPERTENSION***

Coordinatore:

Ch.mo Prof. Palmiero Monteleone

Candidata:

Paola Di Pietro

Tutor:

Ch.mo Prof. Carmine Vecchione

Matricola:

800900034

ANNO ACCADEMICO 2020/2021

TABLE OF CONTENTS

SUMMARY.....	1
1 INTRODUCTION.....	3
1.1 ENDOTHELIAL DYS-FUNCTION AND HYPERTENSION	3
1.1.1 SOURCES AND MECHANISM OF REACTIVE OXYGENS SPECIES GENERATION	5
1.1.2 THE NADPH OXIDASE FAMILY	7
1.1.3 THE MOLECULAR BASIS OF OXIDATIVE STRESS IN HYPERTENSION	8
1.1.4 OXIDATIVE STRESS AND ENDOTHELIAL DYSFUNCTION IN HYPERTENSION: CURRENT EVIDENCE.....	9
1.2 SORTILIN: “STATE OF THE ART”	11
1.2.1 GENETIC RELATIONSHIP BETWEEN THE SORTILIN LOCUS AND CARDIOVASCULAR DISEASES.....	14
1.2.2 THE MULTIFACETED ROLE OF SORTILIN IN CARDIOVASCULAR RISK FACTORS AND CARDIOVASCULAR DISEASES	15
2 AIM.....	19
3 RESULTS	20
3.1 SORTILIN INDUCES ENDOTHELIAL DYSFUNCTION THROUGH INCREASED OXIDATIVE STRESS.	20
3.2 SORTILIN INDUCES ENDOTHELIAL DYSFUNCTION BY ALTERING SPHINGOLIPID METABOLISM.	23
3.3 INHIBITION OF S1P RECEPTOR 3 (S1P3) PREVENTS SORTILIN-INDUCED ENDOTHELIAL DYSFUNCTION AND VASCULAR OXIDATIVE STRESS.	25
3.4 SORTILIN INDUCES VASCULAR OXIDATIVE STRESS BY PROMOTING RAC1-DRIVEN ACTIVATION OF NOX2.....	28
3.5 PKC ϵ ACTS AS A DOWNSTREAM MODULATOR OF S1P3 TO MEDIATE SORTILIN-INDUCED VASCULAR INJURY.	30

3.6 S1P3- OR GP91PHOX-DEFICIENCY PROTECTS FROM ARTERIAL HYPERTENSION AND ENDOTHELIAL DYSFUNCTION EVOKED IN VIVO BY SORTILIN ADMINISTRATION.....	32
3.7 HYPERTENSIVE PATIENTS WITH ENDOTHELIAL DYSFUNCTION HAVE ELEVATED PLASMA LEVELS OF SORTILIN.....	34
3.8 SORTILIN LEVELS ARE ASSOCIATED WITH DYSREGULATED SPHINGOLIPID METABOLISM AND OXIDATIVE STRESS IN HUMANS WITH ARTERIAL HYPERTENSION.....	35
4 DISCUSSION	38
5. CONCLUSIONS.....	45
6. MATERIALS AND METHODS.....	48
6.1 REAGENTS	48
6.2 MICE	48
6.2.1 <i>Vascular reactivity studies</i>	49
6.2.2 <i>Gene silencing</i>	50
6.2.3 <i>Nitric oxide detection</i>	51
6.2.4 <i>Evans blue Dye</i>	52
6.2.5 <i>In vivo sortilin administration</i>	52
6.2.6 <i>Blood pressure measurements</i>	53
6.3 CELL CULTURE.....	53
6.4 MEASUREMENT OF ROS PRODUCTION	54
6.4.1 <i>Sensitive fluorescent indicator dihydroethidium</i>	54
6.4.2 <i>Evaluation of NADPH-Mediated O₂⁻ Production</i>	54
6.5 FLOW CYTOMETRY	55
6.6 QRT-PCR ANALYSIS	55
6.7 IMMUNOFLUORESCENCE AND CONFOCAL FLUORESCENCE IMAGING	56

6.8 WESTERN BLOT.....	56
6.9 HUMAN SUBJECTS	58
6.9.1 <i>Evaluation of Human Endothelial Function by endoPAT</i>	59
6.9.2 <i>Soluble NOX2-derived peptide ELISA detection</i>	60
6.10 SPHINGOLIPID ANALYSIS BY LC-MS/MS.....	61
6.11 STATISTICS.....	62
7. REFERENCES	65
8. SUPPLEMENTARY FIGURES AND TABLES	72

Summary

Sortilin has been positively correlated with vascular disorders in humans. Previous studies showed that sortilin promotes activation of acid sphingomyelinase (ASMase) and subsequently induces an increase of nicotinamide adenine dinucleotide phosphate (NADPH) oxidase activity in coronary endothelial cells. Although preclinical and clinical investigations have highlighted the critical role of sortilin in the pathogenesis of vascular disorders, no studies have yet evaluated the direct effect of sortilin in the modulation of vascular function. Thus, using pharmacological and genetic approaches, coupled with murine and human samples, we aim to unravel the mechanisms recruited by sortilin in the vascular system. We showed that sortilin induced endothelial dysfunction of mesenteric arteries through the activation of the NADPH oxidase 2 (NOX2) isoform, dysfunction prevented by knockdown of acid sphingomyelinase (ASMase) or sphingosine kinase 1. In vivo, recombinant sortilin administration induced arterial hypertension in wild-type mice. In contrast, genetic deletion of sphingosine-1-phosphate (S1P) receptor 3 and gp91phox/NOX2 resulted in preservation of endothelial function and blood pressure homeostasis after 14 days of systemic sortilin administration. Translating these research findings into the clinical setting, we detected elevated sortilin levels in hypertensive patients with endothelial dysfunction. Furthermore, in a population-based cohort of 270 subjects, plasma

levels of sortilin, ASMase activity, and S1P and sNOX2-dp levels were found increased in hypertensive subjects as compared to normotensive controls, being more pronounced in hypertensives with uncontrolled blood pressure.

In conclusion, this study uncovers a previously unknown mechanism underpinning the role of sortilin in the dysregulation of sphingolipid metabolic pathway and NOX2-derived oxidative stress to impair vascular function and blood pressure homeostasis. Furthermore, we suggest the potential of sortilin and its mediators as novel biomarkers for the prediction of vascular dysfunction and high blood pressure (Di Pietro et al. 2022).

1 INTRODUCTION

1.1 Endothelial Dys-function and Hypertension

Hypertension is the most important modifiable risk factor for all-cause morbidity and mortality worldwide and is associated with an increased risk of cardiovascular diseases (Oparil et al. 2018). It is defined as the presence of chronically elevated systemic arterial or diastolic blood pressure equal to or higher than 140 mm Hg and 90 mm Hg, respectively (Weber et al. 2014). Due to its complex pathophysiology, hypertension is described as a multisystem disorder that involves interplay among many factors, including genetic, environmental, endocrine, humoral, and hemodynamic factors, all of which have been described in the Mosaic theory by Page in 1949 (Oparil et al. 2018). Since then, numerous studies have been conducted in an attempt to unravel the multitude of cellular processes involved in the pathogenesis of hypertension. Although the precise cause-effect relationship controversy, a wide range of evidence supports the hypothesis that endothelial dysfunction may contribute to hypertension development. As reported by Panza and colleagues, the impaired endothelium-dependent vasodilator response to acetylcholine was largely related to decreased NO bioactivity (Panza et al. 1995). Moreover, endothelial dysfunction correlated with the severity of hypertension. Consistent with this, patients with uncontrolled

hypertension show a greater impairment of endothelial function compared to controlled hypertension ones (Park et al. 2001).

Once considered a permeable barrier between the bloodstream and the outer vascular wall, the endothelium is now recognized to be a complex organ, fundamental for the maintenance of the vascular tone and homeostasis (Versari et al. 2009). Indeed, endothelium synthesizes and secretes a variety of anti-atherosclerotic molecules, the most important is nitric oxide (NO), a gaseous molecule generated from the metabolism of L-Arginine by endothelial NO synthase (eNOS), constitutively present in endothelial cells (Taddei et al. 2003). Furthermore, endothelial cells are responsible for the dynamic control of blood vessel, including the transport of nutrients and proteins from the intra- to the extravascular compartments (and vice versa), the modulation of the immune response, the regulation of the balance between procoagulant and anticoagulant factors (Taddei et al. 2003). Normally, once stimulated, endothelium produces and releases NO, which, by diffusing to surrounding cells, stimulates guanylate cyclase to produce cyclic guanosine monophosphate and mediates the relaxation of vascular smooth muscle (Versari et al. 2009). Under certain conditions, such as the presence of cardiovascular risk factors, endothelial cells lose their protective function and become proatherosclerotic cells (Taddei et al. 2003), condition defined with the term "endothelial dysfunction". The common feature of endothelial

dysfunction is a decrease in NO. Indeed, increased superoxide anion and other reactive oxygen species (ROS) have been extensively reported to reduce bioactivity of NO, and in turn promoting endothelial dysfunction and elevated blood pressure (Higashi et al. 2012). In presence of NO bioavailability impairment, the dysfunctional endothelium acts by implementing several physiological pathways, such as the production and release of prostanoids and other mediators including endothelin-1, tromboxane A₂, prostaglandin, all of which are detrimental to the arterial wall (Versari et al. 2009).

1.1.1 Sources and Mechanism of Reactive Oxygens Species generation

Oxidative stress refers to an excess in the levels of ROS - which include the superoxide anion (O₂⁻), hydroxyl radical (OH[·]), and other species such as hydrogen peroxide (H₂O₂) and peroxynitrite (ONOO⁻) - over antioxidants defenses within a biological system.

Thus, as a result of oxidative chain reactions, oxidative stress not only promotes direct and irreversible oxidative damage to macromolecules but also disrupts key redox-dependent signaling processes (Stocker et al. 2004). As such, under normal conditions, proteins undergo to reversible oxidative changes involved in cell homeostasis. In pathological conditions, as a result of oxidative stress, proteins are

targets of irreversible oxidation, which ultimately culminate with cell death (Griendling et al. 2021).

ROS are generated by a variety of cellular processes such as respiration, arachidonic acid pathways, cytochrome p450, xanthine oxidase. One of the most important sources of O_2^- and H_2O_2 in the cardiovascular system is NADPH oxidase (NOX), a family of enzymes whose function is to catalyze the transfer of electrons from the cytosol across membranes (Zhang et al. 2020). In detail, the cascade of reactions catalyzed by these enzymes is the reduction of O_2 to produce O_2^- or H_2O_2 in an NADPH-dependent manner, that leads to the generation of secondary ROS including the reaction of O_2^- with nitric oxide to form $ONOO^-$, iron-catalyzed Fenton reaction to produce OH^- (hydroxyl radical), and peroxidase-catalyzed generation of hypochlorous acid (Bedard et al. 2007). While some effects of NADPH oxidase enzymes are due to protein modification by H_2O_2 , others, such as inactivation of NO that occur in blood pressure regulation, are instead mediated directly by the production of superoxide anion (Lassegue et al. 2010). Other secondary sources of ROS include mitochondrial oxidases, xanthine oxidase, endoplasmic reticular oxidases, and uncoupled nitric oxide synthase (NOS) (Sedeek et al. 2009). Production of NO is normally regulated by activation of 3 isoforms NOS: eNOS (endothelial NOS), and nNOS (neuronal NOS), which are constitutively active in a Ca^{2+} /calmodulin-dependent manner; iNOS (inducible

NOS), that is activated by stress independently of Ca^{2+} (Tejero et al. 2019). While in physiological conditions, in the presence of NADPH and BH_4 (tetrahydrobiopterin), NOS catalyzes L-arginine to form L-citrulline and NO, in oxidizing conditions, eNOS becomes uncoupled to produce vasodeleterious O_2^- instead of vasoprotective NO (Tejero et al. 2019).

1.1.2 The NADPH Oxidase family

The NADPH oxidase family comprises seven isoforms, namely NOX1-5, DUOX1 and DUOX2) each defined by the nature of its core catalytic subunit (the so-called NADPH oxidase (NOX) and dual oxidase (DUOX) subunits, and by five regulatory subunits. Some NOX also requires a small GTPase (Rac1 or Rac2) for their activation. The catalytic subunit consists of a single flavin adenine dinucleotide (FAD) bound to the extended carboxy-terminal tail, and two heme-binding regions attached to histidine residues within the transmembrane region of the protein (Drummond et al. 2011). In detail, NOX1 activity requires p22phox, NOXO1 and NOXA1, and the small GTPase Rac. NOX2 is activated by p22phox, p47phox, p67phox, and Rac. NOX3 is dependent of p22phox and NOXO1. NOX4 requires p22phox, while NOX5, DUOX1, and DUOX2 are Ca^{2+} -responsive and do not require regulatory subunits for their activation (Drummond et al. 2011). Their expression is regulated by several substances, these include: vasoactive agents

(angiotensin and thrombin), growth factors, and pro-inflammatory molecules as well as atherogenic particles (Lassegue et al. 2010). The pattern of distribution of the NOX oxidase members vary in tissue and multiple isoforms are constitutively expressed in each of the predominant cell types of the vascular wall: NOX1, NOX2, NOX4, and NOX5, are expressed in cells of heart, blood vessels, kidney, and brain, and linked to oxidative stress in hypertension (Griendling et al. 2021).

1.1.3 The Molecular Basis of Oxidative Stress in Hypertension

While initial studies have focused on the mechanism of inactivation of NO induced by superoxide, our understanding on how ROS overproduction can modify multiple signaling pathways to promote hypertension has advanced significantly. ROS can influence many signaling molecules involved in the regulation of cardiovascular homeostasis. Among them we can mention transcription factors, membrane channels and metabolic enzymes, stabilize cytoskeletal proteins, Ca²⁺-sensitive, phosphatases, and genes (Griendling et al. 2021). The first hypothesis that NADPH enzymes are key players in hypertension comes from a clinical study conducted in early 1989, in which it was shown that NADPH oxidase activation from neutrophils was enhanced in hypertensive patients compared with that of normal controls (Pontremoli et al. 1989). Only in the later 1996, these clinical findings were tested in experimental models, and, a key role for NOX-dependent

ROS overproduction was reported in Angiotensin (Ang) II–dependent hypertension (Rajagopalan et al. 1996). Since then, the role of oxidative stress in hypertension has been tightly established in several animal models of hypertension, including genetic models.

Many studies suggested that neutralizing ROS may be effective in the early stages of hypertension development. Chronic treatment with the antioxidant N-acetylcysteine (NAC) reduces blood pressure in spontaneously hypertensive rats (SHR), as well as in Rac1 overexpressing mice, thus suggesting that an increase in ROS generation by NADPH oxidases predisposes to hypertension (Hassanain et al. 2007; Pechanova et al. 2006). These findings were corroborated by the observation that chronic antioxidant treatment with the superoxide scavenger tempol also blocks the age-related development of high blood pressure in SHR (Nabha et al. 2005). Furthermore, Ang-II dependent hypertension was significantly reversed by genetic deletion of the NADPH oxidase components p47phox or NOX1 (Matsuno et al. 2005; Dikalova et al. 2005).

1.1.4 Oxidative stress and Endothelial dysfunction in Hypertension:

Current Evidence

Oxidative stress and redox-sensitive signaling have been reported to be the major contributor of impaired endothelium-dependent relaxation, increased arterial

stiffness, enhanced contractility, inflammation, vascular calcification, and remodeling (Touyz et al. 2017). There are many lines of evidence implicating increased vascular oxidative stress in the pathogenesis of hypertension. Touyz et al. showed Ang II as the first vasoactive agent able to induce ROS overproduction in vascular cells (Touyz et al. 2017). In this work, increased ROS production, NOX1 and NOX2 expression were found increased in vessels from Ang II–infused mice and in resistance arteries from hypertensive patients (Touyz et al. 2017). Vaziri et al. demonstrated that oral co-administration of lead and vitamin E as free radical scavenger, protected against vascular oxidative stress and hypertension in rats, as compared with those treated with lead alone (Vaziri et al. 1999).

Genetic or pharmacological inhibition of NOX, as well as ROS scavengers or antioxidants were able to inhibit vascular remodeling, decrease inflammation and preserve endothelial function with reduction of blood pressure levels in animal models of hypertension (Touyz et al. 2001). Numerous studies have shown that overexpression of genes aimed at restoring the imbalance between NO and ROS was able to improve vascular function in animal models of hypertension (Jung et al. 2003; Alexander et al. 1999). Adenoviral-mediated gene transfer of eNOS increase NO bioavailability, restore endothelial function and reduced blood pressure in the stroke-prone spontaneously hypertensive rats (SHRSP) (Miller et al. 2005), while overexpression of the antioxidant defense superoxide dismutase also

reduced blood pressure in the SHR (Chu et al. 2003). Other studies supporting a crucial role of NOX/ROS in regulation of vascular function in humans. Patients with genetic NOX deficiency (chronic granulomatous disease) reported higher flow-mediated dilation, lower intima-media thickness, reduced serum NOX2 activity, and increased NO bioavailability, as compared to controls (Violi et al. 2013). In a recent work, Carrizzo and colleagues showed that the supplementation with AkP05, a novel nutraceutical combination improved endothelial function, reduced blood pressure and, increased NO release acting through the stimulation of eNOS and the reduction of ROS production via NADPH-oxidase inhibition. These findings were further corroborated in humans, where it has been found that AkP05 ameliorated endothelial function, enhanced serum NO levels, and reduced blood pressure levels in hypertensive patients after 4 weeks of treatment (Carrizzo et al. 2020).

Taken together, these studies suggest that a better understanding the mechanisms by which redox signaling regulates vascular function may provide the basis for developing more specific modulation of ROS as therapy for hypertension.

1.2 Sortilin: “State of the Art”

Sortilin is a single-type transmembrane receptor belonging to the vacuolar protein sorting 10 protein (Vps10p) domain receptor family, known to be involved in

substrate trafficking and metabolic regulation (Chen et al. 2019; Lefrancois et al. 2003). The Vps10p domain covers the entire extracellular luminal part of sortilin consisting of an N-terminal peptide segment of 700 residues with a β -propeller structure and a C-terminal chain of ten conserved cysteines important for ligand binding (Pallesen et al. 2020). While it is poorly distributed at the plasma membrane (10%), where it acts as an internalization receptor, approximately 90% of the sortilin protein is found in intracellular compartments (vesicles and trans-Golgi) (Morris et al. 1998).

Sortilin is mainly expressed in neurons, hepatocytes, macrophages, and leukocytes, but also in cardiomyocytes, adipocytes, and endothelial cells (Blondeau et al. 2018). Approximately 90% of the sortilin protein is found in the late Golgi apparatus, where it binds to various cargo proteins and regulates their surface location, secretion, or presecretion degradation in lysosomes. Approximately 10% of sortilin is distributed on the cell membrane, where it acts as an internalization receptor by mediating the entry of multiple proteins for recycling or lysosomal degradation (Blondeau et al. 2018). Sortilin is synthesized with an immature propeptide that is cleaved off in the late part of the trans-Golgi through removal of its N-terminal domain by the pro-convertase furin. This propeptide is necessary for correct folding of mature sortilin and inhibition of premature ligand binding (Munck Petersen et al. 1999). Through intracellular sorting and trafficking, sortilin is able to

regulate the cellular levels and activities of several substrate proteins involved in both physiologic and pathologic processes. Recent studies have demonstrated the existence of different mechanism able to modulate sortilin expression and its biological function at different levels: DNA, mRNA, protein, and functional levels. Mutations, single-nucleotide polymorphisms (SNPs), and DNA methylation in the SORT1 gene can affect the protein at both the expression and function level. Some transcription factors, and several microRNAs (miRNA) can act on sortilin mRNA to alter its expression. Moreover, multiple adaptor molecules regulate the trafficking function of sortilin without altering its expression (Ouyang et al. 2020). During the last years, sortilin, a member of the vacuolar protein sorting 10 (VPS10P) family of receptors, has been positively correlated to vascular and metabolic disorders (Goettsch et al. 2018). Preclinical evidence demonstrated that sortilin promotes insulin resistance in type 2 diabetes mellitus and dyslipidaemia by altering hepatic apolipoprotein B-100 metabolism (Strong et al. 2012; Li et al. 2015). Sortilin has been also implicated in vascular calcification and inflammation by favoring the development of arterial atherosclerosis (Mortensen et al. 2014; Goettsch et al. 2016). Furthermore, circulating sortilin levels were found associated with higher risk of major adverse cerebrovascular and cardiovascular events (MACCE), coronary artery disease and peripheral arterial disease (Goettsch et al. 2017; Oh et al. 2017; Biscetti et al. 2019). To date, the cardiovascular effects of

sortilin have been mostly linked to altered circulating cholesterol levels (Linsel-Nitschke et al. 2010; Kjolby et al. 2010; Zeller et al. 2012; Cheng et al. 2017).

However, growing evidence suggests that sortilin may contribute to the pathogenesis of cardiovascular diseases independently of its role in lipid metabolism (Goettsch et al. 2016; Mortensen et al. 2014; Goettsch et al. 2017), pointing to the existence of alternative mechanisms of action.

1.2.1 Genetic relationship between the Sortilin locus and cardiovascular diseases

Sortilin is encoded by the *SORT1* gene located in the 1p13.3 region (Linsel-Nitschke et al. 2010; Petersen et al. 1997). The *SORT1* locus has been independently associated with several cardiac phenotypes, including coronary artery disease, early-onset myocardial infarction, abdominal aortic aneurism, coronary stenosis, coronary artery calcification, and aortic valve calcification (Jones et al. 2013; Smith et al. 2014; Myocardial Infarction Genetics et al. 2009; Wallace et al. 2008).

Although somewhat controversial, a number of genome-wide association studies (GWAS) revealed a strong association between the *SORT1* gene and circulating low density lipoprotein cholesterol (LDL-C) levels (Samani et al. 2007; Kathiresan et al. 2007), supporting a crucial role of sortilin in cholesterol metabolism in humans. Consistent with these findings, *Sort1*-deficient mice were protected

against high cholesterol atherogenic diet-induced liver injury (Li et al. 2017). Other studies reported that the presence of the minor allele of single-nucleotide polymorphism (SNP) rs646776 associated with increased hepatic mRNA expression of *Sort1*, and this correlated negatively to LDL-C in human liver samples (Kathiresan et al. 2008; Musunuru et al. 2010). The major allele of the SNPs rs599839, rs646776, rs629301, and rs12740374, were found to be associated with lower hepatic expression of *SORT1* and elevated LDL-C (Kjolby et al. 2015). On the contrary, the minor allele of rs599839 and rs646776 were associated with decreased LDL-C and reduced risk of both myocardial infarction and coronary artery stenosis (Wang et al. 2011; Muendlein et al. 2009). Although the detailed molecular mechanisms by which sortilin influences both the hepatic and plasma lipid metabolism have not yet been elucidated, recent studies suggested that it clearly impacts ApoB100 secretion, LDL clearance, and foam cell formation (Nurnberg et al. 2016).

1.2.2 The Multifaceted Role of Sortilin in Cardiovascular Risk

Factors and Cardiovascular Diseases

Preclinical studies suggested sortilin as a critical regulator of various processes of atherogenesis, being involved in the development of arterial wall calcification and

inflammation (Mortensen et al. 2014), type II diabetes mellitus (Shi et al. 2005), and dyslipidemia (Kjolby et al. 2010).

Atherosclerosis. Kjolby and colleagues (Kjolby et al. 2015) provided the first experimental evidence for a role of sortilin in atherosclerosis. Using a double knockout model, they showed that loss of both sortilin and low-density lipoprotein receptor (LDLr) reduced atherosclerotic plaque size. This result was later corroborated by Patel et al. (Patel et al. 2015), who demonstrated that, in macrophages, sortilin promotes LDL uptake, foam cell formation, and in turn atherosclerosis. In an elegant study, Mortensen and colleagues demonstrated the ability of sortilin to affect atherogenesis independently of its role in lipid metabolism (Mortensen et al. 2014). In detail, using a mouse model of atherosclerosis, they demonstrated that global deletion of sortilin did not affect circulating cholesterol levels, but reduced the development of both early and late atherosclerotic lesions. The authors also showed that sortilin acts as a high-affinity receptor for the proinflammatory cytokines interleukin-6 (IL-6) and interferon gamma (IFN- γ). Interestingly, the deletion of sortilin in immune cells, such as macrophages and Th1 cells (both of which implicated in atherosclerotic plaque formation) had reduced secretion of IL-6 and IFN- γ . Finally, bone marrow transplant from *Sort1*-deficient mice into *ApoE* knockout mice and fed a Western

diet for 9 weeks reduced atherosclerosis and systemic markers of inflammation (Mortensen et al. 2014).

Vascular calcification. Apart from being considered a hallmark of atherosclerosis, vascular calcification is also considered as an independent predictor of cardiovascular events.

In their work, Goettsch et al. (Goettsch et al. 2018) demonstrated the mechanisms by which sortilin is involved in cardiovascular calcification. Mechanistically, by promoting the trafficking of the tissue-nonspecific alkaline phosphatase protein (TNAP), sortilin mediates the formation of extracellular vesicles with high mineralization competence (Goettsch et al. 2018). In this study, the authors also demonstrated that one of the key mechanisms necessary to induce vascular calcification is post-translational modification of sortilin. In fact, phosphorylation of the sortilin C-terminus by the protein kinases Fam20C or casein kinase 2 accelerates calcification of smooth muscle cell (Goettsch et al. 2018).

Insulin resistance. Recent work suggests that sortilin participates in the dysregulation of hepatic apoB100 metabolism that occur in insulin-resistant conditions (Li et al. 2015). Studies conducted in both mice and cell models reported that sortilin directed intracellular apoB100 for lysosomal degradation in the liver. Increased insulin sensitivity in extrahepatic tissues in *Sort1*^{-/-} mice could be responsible for hepatic lipid accumulation and VLDL secretion during insulin

resistance (Li et al. 2015). Li and coworkers (Li et al. 2015) demonstrated that insulin signaling regulates the protein sortilin through PI3K/AKT-dependent posttranslational mechanisms. This is consistent with previous findings demonstrating that insulin-dependent apoB100 degradation depends on the PI3K signaling and that treatment with wortmannin, the PI3K inhibitor, significantly increases hepatic VLDL production in mice.

The multiple contributions of sortilin to cardiovascular risk suggest this protein as a potential therapeutic target for cardiovascular disease. This hypothesis is also supported by recent evidences showing increased circulating levels of sortilin in patients with coronary artery disease (CAD), and its correlation with the presence and severity of peripheral arterial disease (PAD) in type 2 diabetic patients (Oh et al. 2017; Biscetti et al. 2019).

2 AIM

Until a few years ago, the endothelium was considered a simple selective barrier between the bloodstream and the outer vascular wall, while it is currently recognized as a crucial organ for indispensable for the maintenance of vasomotor balance and vascular homeostasis (Versari et al. 2009), and as such represents the main target of vascular diseases. Furthermore, numerous evidences suggest that the improvement of endothelial function correlates with the reduction of new cardiovascular risk factors.

Although preclinical and clinical investigations have highlighted the critical role of sortilin in the pathogenesis of vascular disorders, so far no studies have investigated a possible direct role of sortilin in the modulation of vascular function.

Thus, the aim of this study was:

1. To determine whether sortilin was able to modulate vascular function in murine models;
2. To assess the effects of sortilin on blood pressure in mice;
3. To evaluate circulating plasma levels of sortilin in patients with endothelial dysfunction and arterial hypertension.

3 RESULTS

3.1 Sortilin induces endothelial dysfunction through increased oxidative stress.

Plasma sortilin level has been associated with a high prevalence of cardiovascular risk factors in patients (Mortensen et al. 2014; Patel et al. 2015). Thus, we first aimed to investigate whether the protein per se was able to influence vascular function. In vascular relaxation studies, sortilin induced a time and dose-dependent impairment of vasodilator response to acetylcholine in mice mesenteric vessels (Figure 1A and Supplemental Figure 1, A and B). As we noted a prominent impairment in vascular reactivity already after 60 min of sortilin preincubation with 2.5 ng/mL, we used this setting for all subsequent experiments. Sortilin impaired neither smooth muscle vasorelaxation evoked by nitroglycerin nor the vasoconstrictive response induced by the thromboxane A₂ receptor agonist U46619 (Supplemental Figure 1, C and D), which suggests that the endothelium is the target of sortilin's vascular action. Nitric oxide (NO) is the most important endothelial-derived factor responsible for the maintenance of vascular function (Katusic et al. 2014). In mesenteric arteries, sortilin caused a marked reduction of NO levels without affecting phosphorylation of endothelial nitric oxide synthase (eNOS) at both Ser1177 and Thr494 (Figure 1, B and C), positive and negative

regulatory sites of the enzyme, respectively (Yuan et al. 2016). The increase in ROS production and the finding that endothelial dysfunction was prevented by the pretreatment with the antioxidant Tempol (Figure 1, D and E), suggesting oxidative stress as the major determinant of reduced NO bioavailability in response to sortilin.

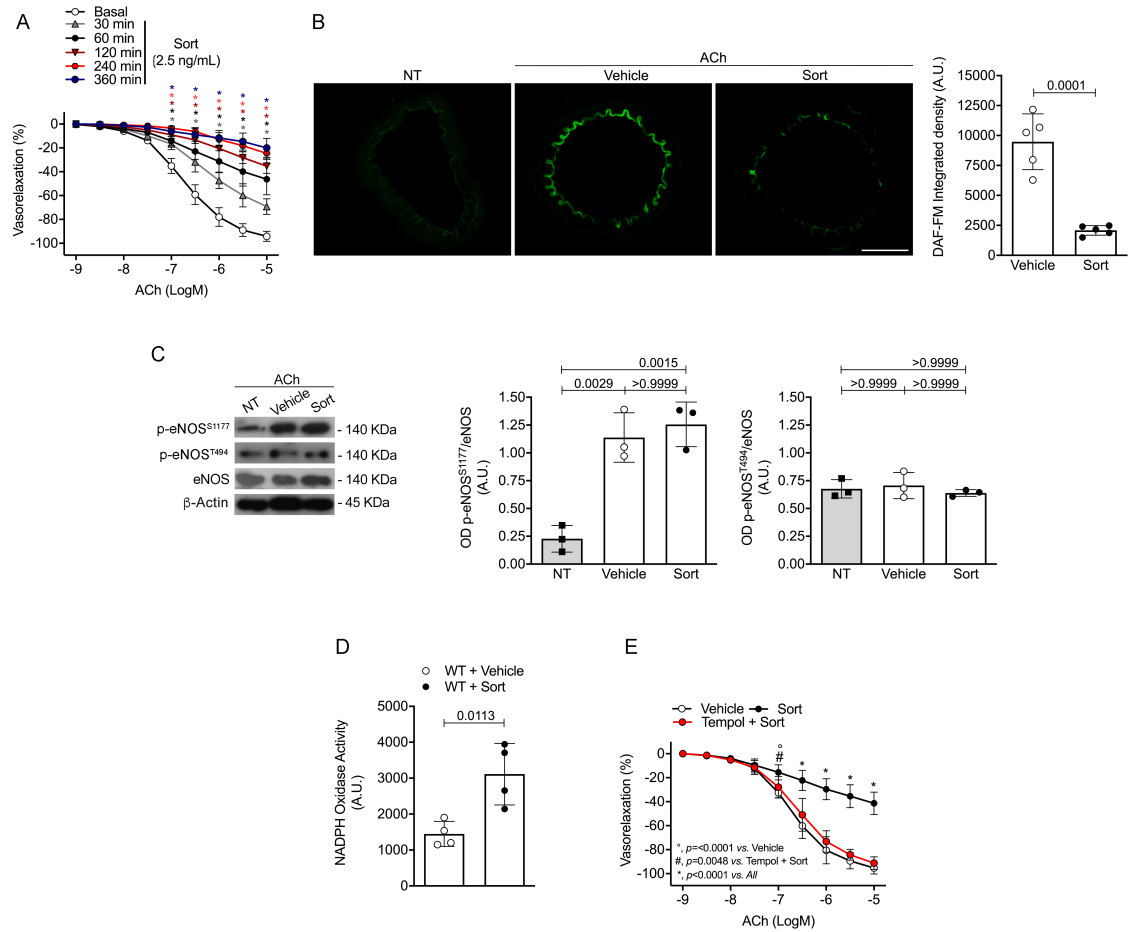


Figure 1. Sortilin impairs endothelium-dependent vasorelaxation through increased ROS production. (A) Acetylcholine (ACh)-evoked vasorelaxation in WT mesenteric arteries exposed to vehicle or sortilin (sort) at 2.5 ng/mL for different preincubation times. (B) Detection of NO by DAF-FM fluorescence in untreated WT mesenteric arteries (NT), stimulated with vehicle or after pretreatment with sort. Scale bar: 50 μ m. DAF-FM fluorescence integrated density in the endothelial layer. A.U., arbitrary units of fluorescence. (C) Representative immunoblots and densitometric analyses evaluating protein levels of phospho-Ser1177-eNOS, phospho-Thr494-eNOS, and total eNOS expression in untreated WT mesenteric arteries (NT), stimulated with ACh alone (vehicle) or after pretreatment with sort for 60 minutes. (D) Effect of sortilin on NADPH oxidase activity in WT mesenteric arteries. Data expressed as increase of chemiluminescence per minute in arbitrary units. (E) ACh-evoked vasorelaxation in WT mesenteric arteries exposed to vehicle, sortilin alone, or pretreated with Tempol for 30 minutes prior to sortilin. Results are expressed as mean \pm SD. (A) * $P < 0.0001$ vs. Basal at the same ACh concentration (as indicated by colour code).

3.2 Sortilin induces endothelial dysfunction by altering sphingolipid metabolism.

Acid sphingomyelinase (ASMase) is a lipid hydrolase that cleaves sphingomyelin to produce bioactive sphingolipids. Previous mechanistic studies have reported that, in response to Fas stimulation, sortilin promotes trafficking and exposure of lysosome-targeted ASMase to the cell membrane surface, a process leading to lipid rafts clustering and assembly of NADPH oxidase (Jin et al. 2008; Bao et al. 2010). In HUVEC cells, we show that sortilin evoked, *per se*, NADPH oxidase activation and increased intracellular ASMase activity (Figure 2, A and B). Small interfering RNA (siRNA)-mediated knockdown of ASMase effectively protected against endothelial dysfunction as well as NADPH-derived ROS overproduction in mesenteric arteries as compared to scrambled siRNA after sortilin exposure (Figure 2, C and D), thus unravelling the critical role played by ASMase in the vascular effects of sortilin. Ceramide is the immediate metabolic product of ASMase action, which can be further modified to form complex sphingolipids or broken down into sphingosine and free fatty acids by ceramidases (Castro et al. 2014). We next investigated whether sphingosine or its precursor ceramide mediates the deleterious effect of sortilin. Knockdown of the acid ceramidase (aCDase), responsible for sphingosine generation by cleavage, effectively protected from sortilin-evoked endothelial dysfunction (Supplemental Figure 2A), thus demonstrating that sphingosine, but

not ceramide, is responsible for the endothelial injury induced by sortilin. To determine whether sphingosine or its phosphorylated derivative S1P could be accountable for the sortilin-dependent NADPH oxidase activation pathway, we investigated the potential contribution of sphingosine kinases (SphKs) 1 and 2, which generate the endogenous mediator S1P. Interestingly, only pharmacological inhibition of SphK1 with SK1-I or its genetic suppression protected against sortilin-induced endothelial dysfunction and superoxide generation in HUVECs, whereas these effects were not observed after inhibition of SphK2 with either K145 or siRNA-mediated knockdown (Figure 2, E and F; Supplemental Figure 2, B and C). Remarkably, quantification of sphingolipid levels by LC-MS/MS in sortilin-treated endothelial cells showed a consistent decrease in intracellular ceramide content, including cer-C16, cer-C18, cer-C22, cer-C24 and cer-C24:1 (Supplemental Figure 2D), that was paralleled by increased extracellular S1P levels (Figure 2G). This indicates that sortilin drives the activation of the ASMase/aCDase pathway, leading to an altered rheostat in favour of S1P at the expense of ceramide. We then explored whether depletion of ceramides rather than accumulation of S1P is responsible of endothelial dysfunction caused by sortilin. The results showed that neither C16- nor C18-ceramides pretreatment (10 nM) was able to prevent sortilin vascular effect, while the pretreatment with aCDase small interfering RNA

protected from endothelial dysfunction induced by sortilin (Supplemental Figure 2, E and F).

Besides corroborating a dysregulated sphingolipid signaling in the endothelium, these data suggest that strategies aimed to restore ceramide levels are ineffective to prevent the endothelial dysfunction evoked by sortilin unless coupled with blocking of the generation of sphingosine and its derivative active form.

3.3 Inhibition of S1P receptor 3 (S1P3) prevents sortilin-induced endothelial dysfunction and vascular oxidative stress.

Given the importance of S1P1 and S1P3 in the regulation of the vascular tone of resistance vessels (Cantalupo et al. 2017), we next investigated their role in sortilin signaling pathway. Sortilin caused an up-regulation of S1P3, but not S1P1 expression, in wild-type (WT) mesenteric arteries (Figure 2H). In HUVECs, sortilin induced a substantial increase in both the percentage of cells expressing the receptor (% of positive cell) and S1P3 expression amount after 30 minutes of stimulation, whereas at later time points, a downregulation of the receptor (both in terms of percentage and amount) was observed (Supplemental Figure 3, A and B). Measurement of mRNA relative expression of S1P3 at different time points revealed that sortilin induced a progressive increase of S1P3 de-novo synthesis, starting from 60 minutes up to 360 minutes (Supplemental Figure 3C). Thus, via

S1P, sortilin induced S1P3 activation through a first round of mobilization of the reserve pool of receptors followed by the induction of de novo synthesis pool in a time-dependent manner. Inhibition of S1P3 with TY52156 prevented sortilin-induced endothelial dysfunction as well as oxidative stress in mesenteric arteries and HUVECs, whereas these effects were not observed after S1P1 inhibition with W146 (Figure 2, I and J; Supplemental Figure 4, A and B). Consistently, mesenteric arteries from S1P3-deficient mice were completely protected against sortilin-induced ROS production and endothelial dysfunction (Figure 2, K and L), clearly supporting the thesis that S1P3 mediates the crosstalk between S1P and NADPH oxidase and sortilin deleterious effects.

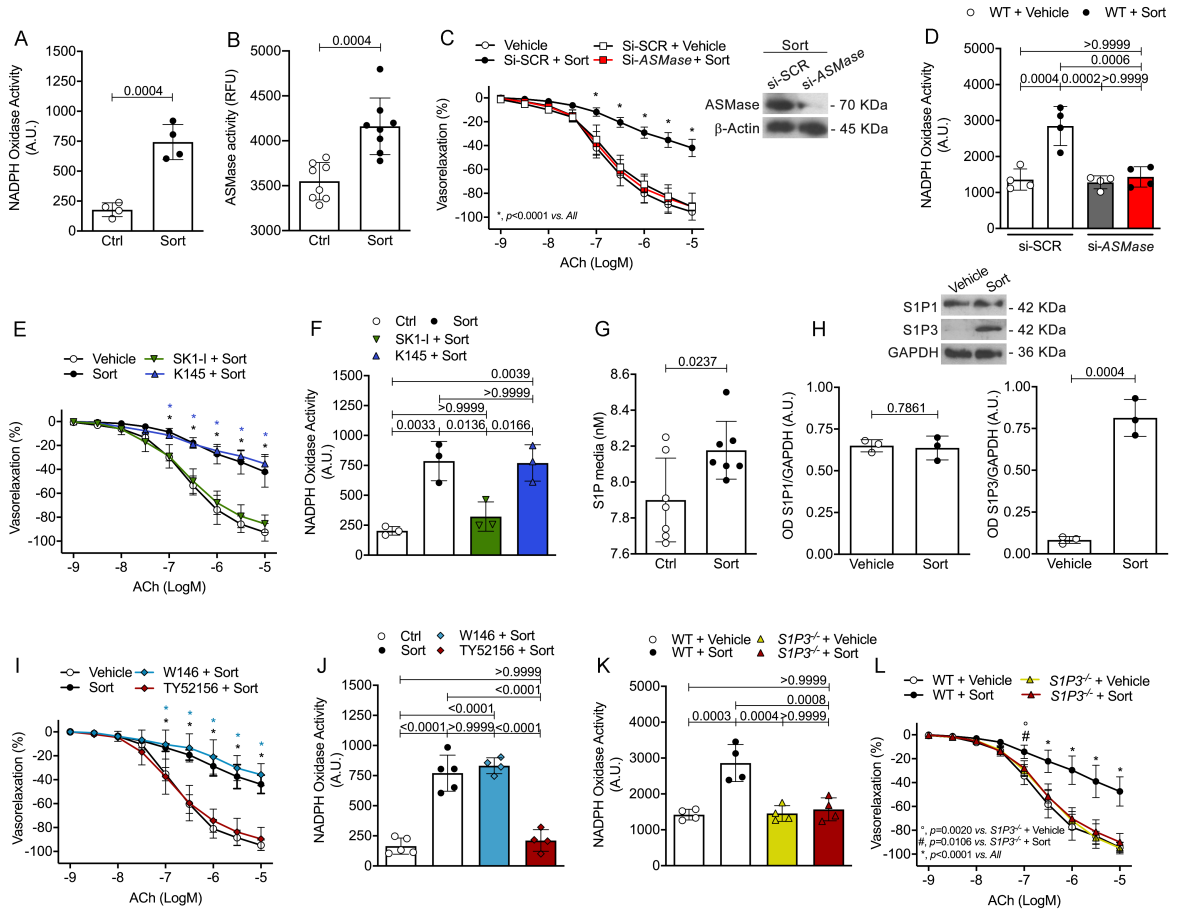


Figure 2. Sortilin evokes endothelial dysfunction through the S1P signaling pathway. (A) NADPH oxidase activity and (B) ASMase activity (RFU, relative fluorescence units) in HUVECs treated with vehicle (ctrl) or sortilin. (C) ACh-evoked vasorelaxation in WT mesenteric arteries exposed to vehicle, or pretransfected with siRNA against acid sphingomyelinase (si-ASMase) before sortilin; scrambled siRNA (si-SCR) was used as control. Representative immunoblots showing ASMase protein levels after siRNA silencing. (D) Effect of si-ASMase on NADPH oxidase activity in WT mesenteric arteries exposed to sortilin. (E) ACh-evoked vasorelaxation in WT mesenteric arteries exposed to vehicle, sortilin, or pretreated with either K145 or SK1-I. (F) Effects of K145 and SK1-I on NADPH oxidase activity in sortilin-stimulated HUVECs. (G) LC-MS/MS quantification of extracellular S1P levels in HUVECs treated with vehicle (ctrl) or sortilin. (H) Representative immunoblots and densitometric analyses evaluating S1P1 and S1P3 expression in WT mesenteric arteries exposed to vehicle or sortilin. (I) ACh-evoked vasorelaxation in WT mesenteric arteries exposed to vehicle, sortilin, or pretreated with either W146 or TY52156 before sortilin. (J and K) NADPH oxidase activity in (J) HUVECs treated with vehicle (ctrl), sortilin, or pretreated with either W146 or TY52156 before sortilin and in (K) S1P3^{-/-} mesenteric arteries exposed to vehicle or sortilin. (L) ACh-evoked vasorelaxation in mesenteric arteries from WT and S1P3^{-/-} mice exposed to vehicle or sortilin. Results are expressed as mean \pm SD. (E) * $P < 0.0001$ vs. Vehicle or SK1-I + Sort at the same ACh concentration (as indicated by colour code). (I) * $P < 0.0001$ vs. Vehicle or TY52156 + Sort at the same ACh concentration (as indicated by colour code).

3.4 Sortilin induces vascular oxidative stress by promoting Rac1-driven activation of NOX2.

Upon activation, the NADPH oxidase complex undergoes post-translational modifications of its oxidase regulatory subunits, allowing association with the membrane catalytic subunit. Also, some NADPH oxidase isoforms (NOX) require a small GTPase (Rac1 or Rac2) for their activation (Drummond et al. 2011). In endothelial cells, sortilin promoted Rac1 activation, as demonstrated by translocation of the latter to the plasma membrane, an effect prevented by pretreatment with the S1P3 inhibitor TY52156 (Figure 3A). Of note, the use of Rac1 inhibitor, NSC23766 was able to prevent the impaired dilator response to acetylcholine evoked by sortilin (Figure 3B). We next determined the individual contribution of different NOX isoforms in sortilin-induced vascular oxidative stress. NOX2 inhibition by GSK2795039 effectively prevented endothelial dysfunction as well as oxidative stress induced by sortilin, whereas these effects were not observed with the NOX1 inhibitor ML171 (Figure 3, C and D). Sortilin-induced superoxide generation and NO reduction were prevented by both superoxide dismutase–polyethylene glycol (PEG-SOD), a potent scavenger of oxygen free radicals, and gp91 ds-tat, a specific peptide that blocks NOX2 assembly and activation (Supplemental Figure 5, A-D). Remarkably, mesenteric arteries from NOX2-deficient mice (gp91^{phox^{-/-}}) were significantly protected against

sortilin-induced NADPH oxidase activation and endothelial dysfunction (Figure 3, E and F). These results clearly indicate NOX2 as the effector of sortilin-mediated vascular oxidative stress via the ASMase/S1P/S1P3 axis.

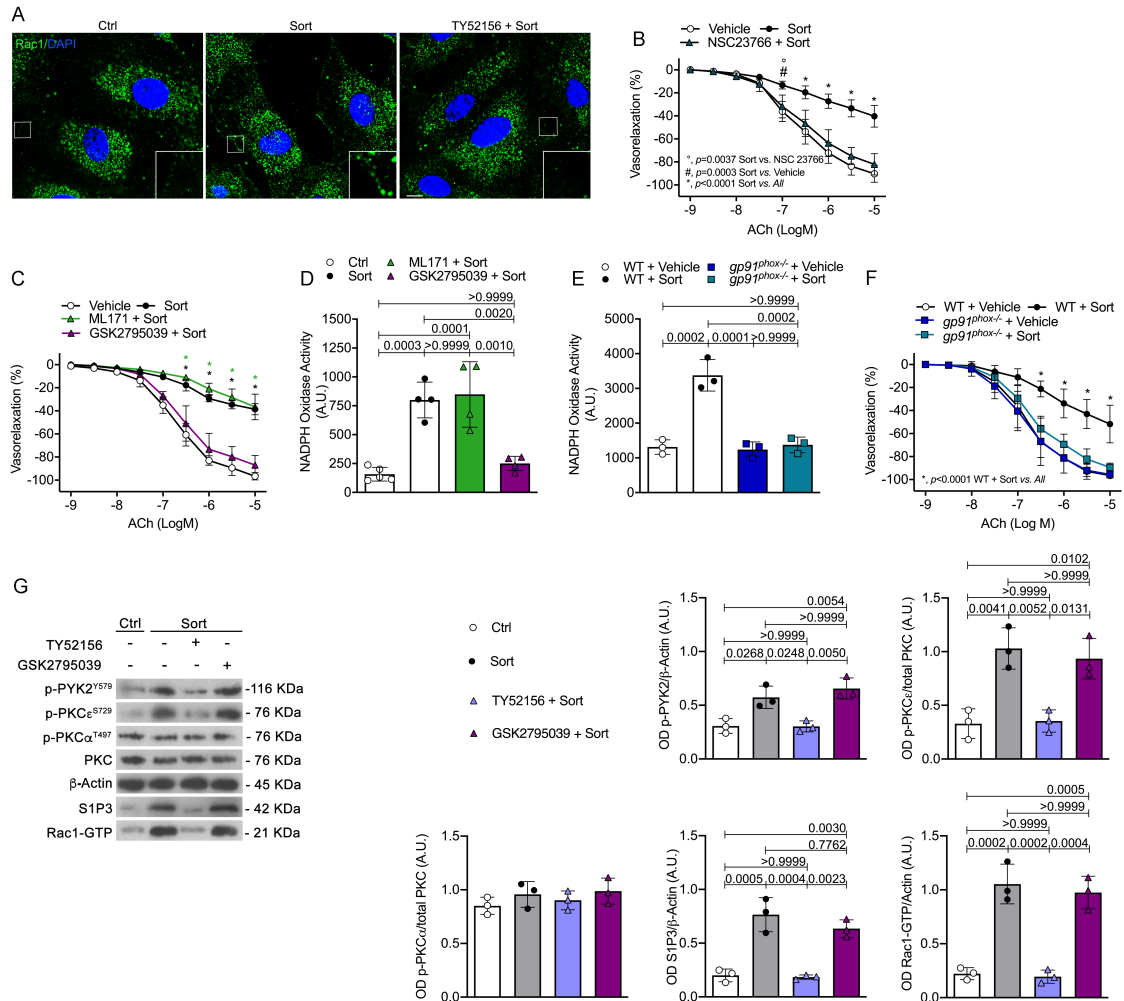


Figure 3. Phosphorylation of PKC ϵ and PYK2 is required for Rac1-dependent NOX2 activation. (A) Immunofluorescence staining of Rac1 in HUVECs treated with vehicle (ctrl), sortilin, or pretreated with the S1P3 inhibitor TY52156. Arrows: membrane translocation of Rac1. Scale bar: 10 μ m. (B) ACh-evoked vasorelaxation in mesenteric arteries exposed to vehicle, sortilin alone or in the presence of NSC23766. (C) ACh-evoked vasorelaxation in mesenteric arteries pretreated with ML171 or GSK2795039. (D) NADPH oxidase activity in HUVECs; vehicle (ctrl), sortilin, or pre-incubated with ML171 or GSK2795039. (E) NADPH oxidase activity in WT and *gp91phox*^{-/-} mesenteric arteries. (F) ACh-evoked vasorelaxation in mesenteric arteries from WT and *gp91phox*^{-/-} mice. (G) Immunoblots and densitometric analyses of phospho-PYK2, phospho-PKC ϵ , phospho-PKC α , PKC, S1P3, and Rac1-GTP in HUVECs; vehicle (ctrl) or sortilin in the presence or absence of TY52156 or GSK2795039. Results are expressed as mean \pm SD. (C) * $P < 0.0001$.

3.5 PKC ϵ acts as a downstream modulator of S1P3 to mediate sortilin-induced vascular injury.

To define the mechanism by which the interaction of sortilin and S1P3 activates the Rac-1 machinery, we investigated the potential involvement of two protein kinase C (PKC) isoforms and proline-rich tyrosine kinase 2 (PYK2), which have been previously implicated in ROS production (Poolman et al. 2013; Lin et al. 2016; Inoguchi et al. 2003).

In HUVECs, sortilin did not cause activation of PKC α (T497), while it increased phosphorylation of PKC ϵ (S729) and PYK2 (Y579) (Figure 3G). Selective inhibition of S1P3 with TY52156 prevented activation of PKC ϵ , PYK2, and Rac1-GTP, whereas pretreatment with NOX2 inhibitor GSK2795039 did not (Figure 3G).

Coherently, sortilin induced phosphorylation of PKC ϵ and PYK2 in mesenteric arteries from WT and gp91^{phox}^{-/-} mice, but not from S1P3-deficient mice (Figure 4A). Of note, knockdown of PKC ϵ abolished sortilin-induced endothelial dysfunction in WT mice mesenteric arteries (Figure 4B) as well as activation of PYK2 and Rac1 (Figure 4C). These findings strongly support the notion that PKC ϵ participates in sortilin signaling, acting as a downstream effector of S1P3 and an upstream modulator of PYK2 and Rac1.

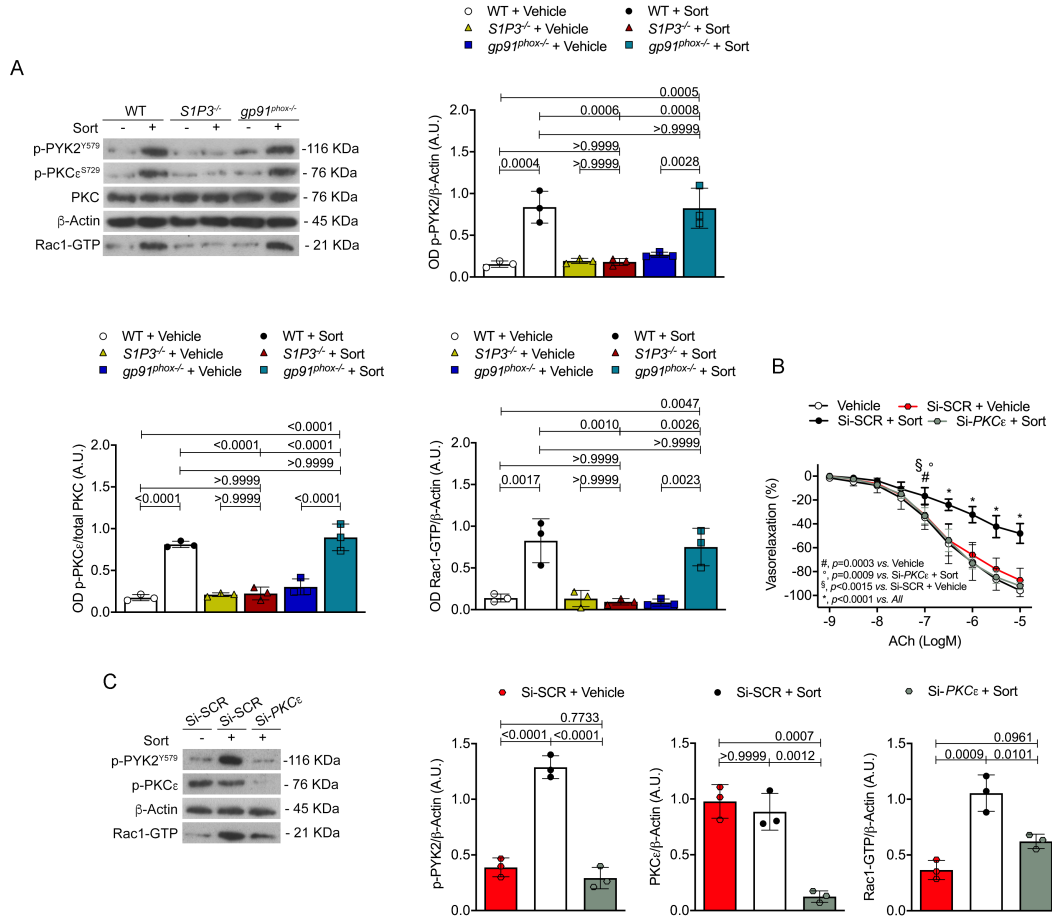


Figure 4 PKC ϵ is involved in sortilin-induced vascular damage. (A) Representative immunoblots and densitometric analyses of 3 independent experiments evaluating protein levels of phospho-PYK2, phospho-PKC ϵ , and Rac1-GTP in WT, S1P3 $^{-/-}$, and gp91 phox $^{-/-}$ vessels exposed to vehicle or sortilin for 60 minutes. (B) ACh-evoked vasorelaxation in WT mesenteric arteries exposed to vehicle, or pretransfected with either siRNA silencing PKC ϵ or a scrambled siRNA (si-SCR) and then exposed to sortilin for 60 minutes. (C) Representative immunoblots and densitometric analyses of 3 independent experiments evaluating phospho-PYK2, and Rac1-GTP levels in WT mesenteric arteries pretransfected with either siRNA silencing PKC ϵ or a scrambled siRNA (si-SCR) and then exposed to sortilin; the effectiveness of PKC ϵ silencing was determined by western blotting. Results are expressed as mean \pm SD.

3.6 S1P3- or gp91phox-deficiency protects from arterial hypertension and endothelial dysfunction evoked in vivo by sortilin administration.

Oxidative stress and endothelial dysfunction are strongly associated with hypertension (Khan et al. 2001; Dandona et al. 2000; Schulz et al. 2011). Based on the above findings, we assessed the effects of sortilin on blood pressure in vivo. A single administration of recombinant sortilin (40 ng/mL, i.p.) induced a transient increase of blood pressure in WT mice; the effect persisted for 4 hours, with near-baseline levels returning within 6 hours from treatment (Supplemental Figure 6A). When we excised vessels for vascular reactivity studies, we observed endothelial dysfunction in WT vessels (Supplemental Figure 6B). In contrast, administration of sortilin did not promote blood pressure increase and vascular dysfunction in either S1P3- or gp91^{phox}-deficient mice (Supplemental Figure 6, C-F). Notably, a single injection of the S1P3 inhibitor TY52156 1 hour from sortilin administration was sufficient to rescue the harmful effect, lowering blood pressure to normal values in WT mice (Supplemental Figure 6G). Western blot analysis confirmed the loss of gp91^{phox} and S1P3 protein expression in mesenteric arteries of both strains of mice (Supplemental Figure 6H).

To mimic an in vivo condition of sustained high circulating levels of sortilin, mice were implanted with osmotic pumps delivering recombinant sortilin protein for 14

days. According to the literature (Cantalupo et al. 2017; Jung et al. 2004), genetic deletion of S1P3 or gp91^{phox} does not influence blood pressure levels under basal conditions (Figure 5A). Chronic infusion of sortilin caused a sustained increase in arterial blood pressure in WT mice (Figure 5B). Interestingly, the evaluation of vascular function in mesenteric arteries excised after 14 days of in vivo sortilin treatment revealed there was an impairment of endothelial-dependent vasorelaxation in WT mice vessels (Figure 5E) that was similar to that observed in the experiments in which sortilin was administered in a single administration or in ex vivo. We found that either S1P3- or gp91^{phox}-deficient mice were completely protected from sortilin-evoked blood pressure increase, and endothelial vasorelaxation impairment (Figure 5, C-E). Besides demonstrating the critical involvement of S1P3 and NOX2 in sortilin-mediated high blood pressure, these results also support the hypothesis of a causal role for sortilin-dependent endothelial dysfunction in the development of hypertension.

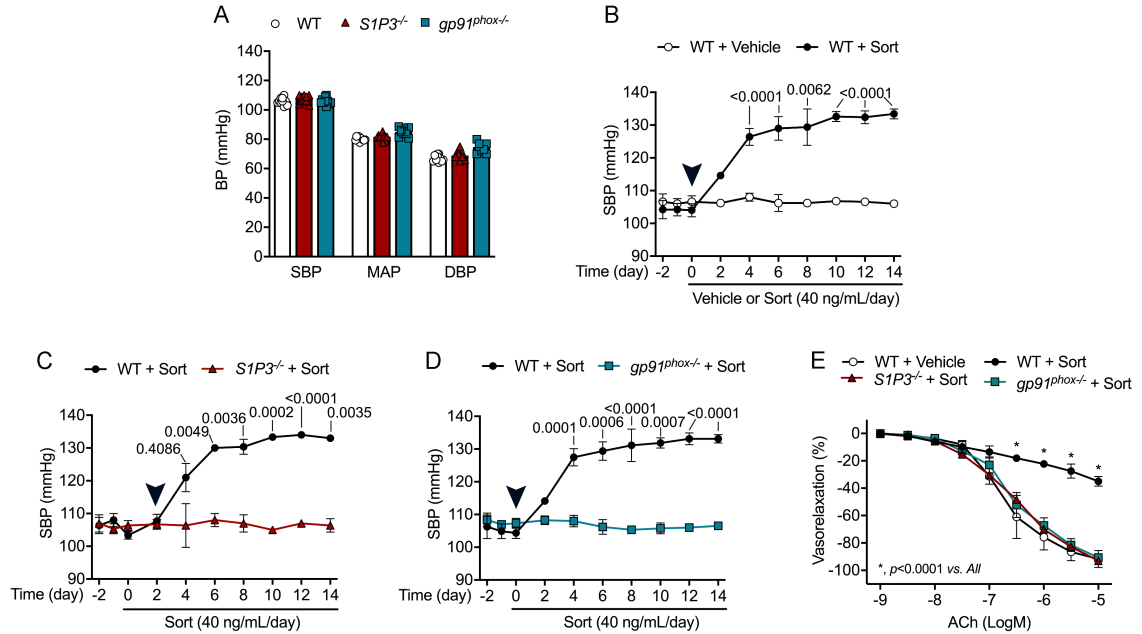


Figure 5 Genetic deletion of either S1P3 or gp91phox protects mice from chronic sortilin-induced high blood pressure and endothelial dysfunction. (A) Baseline of systolic blood pressure (SBP), mean arterial pressure (MAP), and diastolic blood pressure (DBP) measured in WT, S1P3^{-/-}, and gp91phox^{-/-} mice. (B-D) Time courses of SBP measured before and after implantation of an osmotic pump delivering vehicle or sortilin in (B) WT mice, (C) S1P3^{-/-} mice, and (D) gp91phox^{-/-} mice. Arrowheads indicate the day of implantation. (E) ACh-evoked vasorelaxation in mesenteric arteries from WT, S1P3^{-/-}, and gp91phox^{-/-} mice, after 14 days of infusion. Results are expressed as mean ± SD.

3.7 Hypertensive patients with endothelial dysfunction have elevated plasma levels of sortilin.

To translate the experimental findings, we first investigated plasma sortilin concentrations in hypertensive patients belonging to the Campania Salute Network who had undergone endothelial function evaluation. Characteristics of study population are presented in Table 1. As published before (Carrizzo et al. 2020) and shown in our cohort, hypertensive patients showed lower mean reactive

hyperemia index (RHI) compared to healthy subjects (Figure 6A). Interestingly, plasma levels of sortilin were substantially increased in hypertensive patients when compared to normotensive individuals (Figure 6B), thus supporting the relevance of sortilin for endothelial dysfunction in patients with arterial hypertension.

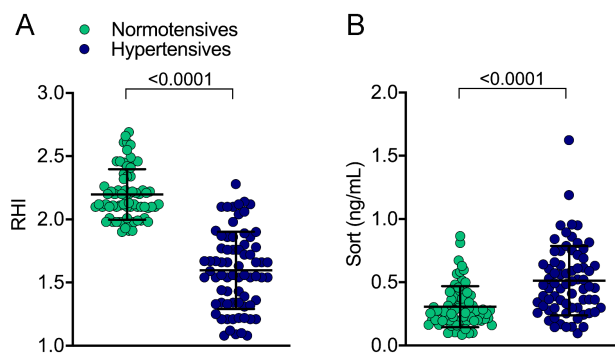


Figure 6 Sortilin levels are elevated in hypertensive patients with endothelial dysfunction. (A) Reactive hyperemia index (RHI) and (B) plasma sortilin levels in normotensive and hypertensive subjects from the Campania Salute Network; (n=71 normotensives, n=71 hypertensives).

3.8 Sortilin levels are associated with dysregulated sphingolipid metabolism and oxidative stress in humans with arterial hypertension.

To strengthen the translational relevance of our findings, we then extended our studies to measure plasma levels of sortilin, S1P, soluble NOX2-derived peptide (sNOX2-dp), and ASMase activity in a large population-based cohort of the Moli-

Sani study. This cohort consisted of hypertensive patients taking antihypertensive medication who were stratified into controlled hypertensives and uncontrolled hypertensives, as well as normotensive control subjects. The clinical and biochemical characteristics are summarized in Table 2. The three groups were strictly matched with respect to age, gender and laboratory characteristics but differed significantly in terms of blood pressure levels. Plasma sortilin, ASMAse activity, S1P, and sNOX2-dp levels were markedly elevated in the entire hypertensive population as compared to healthy controls, and the increase was even more pronounced in hypertensive patients with uncontrolled BP than in controlled hypertensive and normotensive counterparts (Figure 6, C-F). Analysis of variance excluded a potential influence of antihypertensive drug therapy on plasma sortilin concentrations (Supplemental Table 2). Notably, a significant positive correlation was found between circulating sortilin and S1P levels in the entire hypertensive population ($r=0.465$, $P<0.0001$; Figure 6G). We also observed a positive correlation between S1P and sNOX2-dp plasma levels in the same samples ($r=0.3515$; $p<0.0001$; Figure 6H).

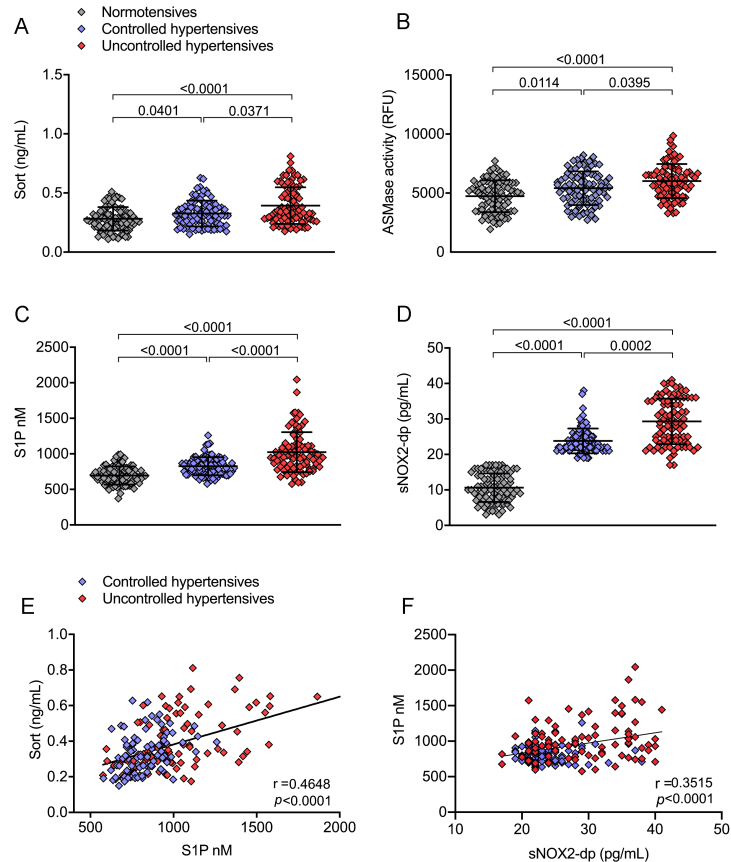


Figure 7 Elevated sortilin levels are associated with sphingolipids dysregulation and oxidative stress in hypertensive patients. Plasma levels of (A) sortilin, (B) ASMase activity (RFU), (C) S1P, and (D) sNOX2-dp in normotensives, controlled and uncontrolled hypertensives from the Moli-Sani Study; ($n=81$ normotensives, $n=91$ controlled hypertensives, $n=90$ uncontrolled hypertensives). (E) Pearson's correlation coefficient analysis between sortilin and S1P plasma levels in the entire hypertensive population. (F) Pearson's correlation coefficient analysis between S1P and sNOX2-dp plasma levels in the entire hypertensive population. Results are expressed as mean \pm SD

4 DISCUSSION

We demonstrate here for the first time the direct role that sortilin has on vascular function. In particular, we found that sortilin promotes endothelial dysfunction and arterial hypertension in mice via a sphingolipid-dependent mechanism.

Additionally, we provided evidence supporting the notion that sortilin plays a pivotal role in dysfunctional sphingolipid metabolism and oxidative stress associated with hypertension in humans.

Previous work has shown some mechanistic insight into the role of sortilin in mediating NADPH oxidase activation (Bao et al. 2010). Using an in vitro model, Bao et al. (Bao et al. 2010) demonstrated that, in response to Fas receptor stimulation, sortilin together with ASMase promote the trafficking of lysosomes toward the cell membranes resulting in clustering of lipid rafts and consequent aggregation of NADPH subunits. Moreover, the decrease in NO levels induced by FasL in isolated bovine coronary arteries was efficiently reversed by sortilin inhibition, an effect similar to that observed with NOX pharmacological inactivation (Bao et al. 2010), thus suggesting a key role of sortilin in the ceramide–redox signaling pathway in endothelial cells.

In the present study, sortilin-induced ROS overproduction and the consequential endothelial dysfunction of resistance vessels were completely prevented by knockdown of ASMase, suggesting that circulating sortilin, *per se*, produces a

deleterious vascular effect by directly promoting ASMase activation. Once activated, the ASMase, translocated to the outer cell membrane, gives rise to ceramide production that, via the activity of SphKs, can be further metabolized into S1P (Pavoine et al. 2009). Owing to the interconvertible nature of these bioactive sphingolipids, the fine balance between anti-proliferative activity of ceramide and anti-apoptotic effects of S1P, also referred to as “sphingolipid rheostat”, is critical for cellular homeostasis (Spiegel et al. 2003). Even though studies conducted over the last decade substantially extended our knowledge in the context of sphingolipids’ origin and metabolism, many fundamental questions about the mechanisms underlying both their homeostasis and dysregulation remain to be solved. In addition to red blood cells, endothelial cells actively produce and release S1P into the bloodstream, thus representing an additional important source of plasma S1P (Xiong et al. 2014). Its effects are mostly mediated by the activation of five high-affinity G-protein-coupled receptors, namely S1P1–5 (Chun et al. 2010), whose cellular and temporal expression has been proposed as a critical determinant for their specific roles in various organ systems. Among these, S1P1, S1P2 and S1P3 receptors are the major subtypes in the cardiovascular system (Machida et al. 2016). Although previous studies have shown that S1P exerts vasculoprotective effects (Tolle et al. 2008; Cantalupo et al. 2017), our data provide strong evidence that in response to sortilin, ASMase-mediated NADPH oxidase

activation requires the action of S1P. It is important to underline that unlike previous studies evaluating in vitro or ex vivo vascular cell responses following exogenous S1P stimulation (Nofer et al. 2004; Cantalupo et al. 2017), here we examined the effects evoked by the modulation of endogenous S1P levels. Thus, in our experimental condition, the adverse effects of S1P on endothelial cells may be due to the alternative sphingolipid metabolic pathway dependent on ASMase activation, that results in an altered rheostat in favour of S1P at the expense of ceramide.

Through a pharmacological approach, we identified S1P3 as the key S1P receptor mediating the vascular effects evoked by sortilin. In agreement, S1P3-deficient vessels were completely protected against sortilin-induced endothelial dysfunction and ROS overproduction.

It is generally accepted that Rac1 plays a critical role for activation of NADPH oxidase complex. Herein, we also established the recruitment of Rac1 into the signaling cascade leading to ROS generation in response to sortilin, an effect mediated by NADPH oxidase isoform 2, since its deficiency prevented sortilin-induced ROS production as well as endothelial dysfunction in mice mesenteric resistance arteries.

Protein kinase C (PKC) is a critical player that contributes to the regulation of vascular system under both physiological and pathophysiological conditions

(Mochly-Rosen et al. 2012). Previous works have indicated PKC activation as a relevant pathway responsible for NADPH oxidase activation in vascular tissues (Inoguchi et al. 2003; White et al. 2009). Of interest, Lin and colleagues (Lin et al. 2016), demonstrated the ability of S1P to induce ROS generation via a direct cooperation between PKC and proline-rich tyrosine kinase 2 (PYK2). Among PKC isoforms, both PKC α and PKC ϵ have been reported to participate in PYK2 activation (Cheng et al. 2002; Bayer et al. 2003). These reports led us to investigate the intracellular signaling events between S1P3 and NOX2-dependent ROS production, focusing especially on PKC pathway. In isolated endothelial cells, sortilin caused activation of PKC ϵ and PYK2, an effect blunted by TY52156 pretreatment but not with the NOX2 inhibitor. These findings were strongly supported by the fact that, in contrast with sortilin-treated WT and gp91^{phox-/-} vessels, the effect was absent in S1P3^{-/-} vessels, an observation clearly identifying, on the one hand, PKC ϵ and PYK2 as downstream effectors of S1P3, and upstream regulators of the Rac1/NOX2 pathway on the other. Taken together, our results have unmasked a novel molecular mechanism underpinning the role of sortilin in the sphingolipid dysregulation, oxidative stress and endothelial dysfunction in the pathophysiology of vascular complications.

Although endothelial dysfunction has long been considered as a detrimental effect of high blood pressure, there is now compelling evidence that vascular oxidative

stress has a causal role in the pathogenesis of hypertension (Khan et al. 2001; Dandona et al. 2000; Schulz et al. 2011). In this regard, studies in human resistance vessels transfected with gp91^{phox} antisense oligonucleotides (Touyz et al. 2002), as well as in endothelial cell-specific NOX2 knockout mice (Sag et al. 2017), have demonstrated the undeniable contribution of NOX2-derived oxidative stress to the development of hypertension.

Since mesenteric arteries represent the prototype of resistance vessel for blood pressure regulation, we investigated the effects of sortilin in acute and chronic administration paradigms in vivo. Sortilin caused increased blood pressure in WT mice, a hemodynamic effect that was entirely counteracted by deficiency of S1P3 or gp91^{phox}. While acute administration resulted in a transient increase in blood pressure in WT mice, chronic sortilin infusion induced sustained arterial pressure elevation over all the observation period from the third day on. Notably, in both experimental settings, in vivo administration of recombinant sortilin induced endothelial dysfunction, whereas the lack of S1P3 or gp91^{phox} resulted in a strong protective effect against vascular dysfunction. An interesting observation of this study was that the impaired endothelium-dependent relaxation observed with sortilin after in vivo administration was similar to that obtained in vitro, a setting that cannot be influenced by the systemic inflammatory response or sympathetic activation. Thus, these results strongly support the notion that the activation of the

S1P/NOX2 signaling axis induced by sortilin, and the subsequent impairment of endothelial-dependent dilation, may be causally involved in the increased blood pressure detected after in vivo administration of the protein.

Translating our experimental studies to humans, we found that circulating sortilin levels were elevated in hypertensive individuals with impaired endothelial function, thus supporting the hypothesis of its involvement in the pathogenesis or sequelae of hypertension. This finding was further evaluated in a second cohort of individuals without additional comorbidities and stratified by blood pressure level. Even more thrilling, the results emerging from hypertensive stratification revealed that plasma sortilin concentration was higher in hypertensive patients with uncontrolled BP than in controlled hypertensives and the normotensives counterpart. Moreover, plasma levels of ASMase activity, S1P, and sNOX2-dp, key mediators involved in the deleterious effects of sortilin, followed the same modification pattern observed in sortilin circulating levels.

In agreement with the results obtained in mice, demonstrating how sortilin signaling alters sphingolipid metabolism thereby promoting endothelial dysfunction and arterial hypertension, our data in humans suggest that sortilin and its mediators may represent new biomarkers for the prediction of vascular dysfunction and high blood pressure.

This hypothesis is also coherently supported by the positive correlations found in our cohort of hypertensive patients between plasma levels of sortilin and S1P, and between the latter and sNOX2-dp content, thus confirming the interdependency between sortilin, dysregulated sphingolipid metabolism and oxidative stress in humans with arterial hypertension.

5. CONCLUSIONS

This is the first study to provide mechanistic insight in which sortilin orchestrate complex intracellular signaling to control vascular function and blood pressure homeostasis, highlighting sortilin as a new potential target in arterial hypertension (Di Pietro et al. 2022). Moreover, these findings may add new aspects to the pathophysiology of the sphingolipid pathway, revealing the mechanism by which an alternative signaling pathway involving ASMase drives to a dysregulated sphingolipid signaling leading to deregulation of cardiovascular functions. Thus, although sphingolipids are essential regulators of cardiovascular homeostasis, our results could offer a plausible explanation for the altered sphingolipids levels observed in several cardiovascular diseases (Deutschman et al. 2003; Sattler et al. 2014). Few studies have reported the ability of some antihypertensive drugs, including angiotensin II receptor blockers (Spijkers et al. 2011; Polzin et al. 2021), calcium channel- and beta-blockers (Kornhuber et al. 2010), to modulate pathways which integrate into S1P signaling, but to date preclinical and clinical studies investigating the specific interaction between antihypertensives and sphingolipid-related signaling pathways are still lacking. Even though our cohort of hypertensive patients was receiving antihypertensive treatment, we demonstrated that plasma sortilin concentrations were not influenced by drug therapy.

Despite the efficacy of current drug treatments, the difficulty in achieving the optimal BP levels by a large percentage of hypertensive patients reveals the importance to develop new preventive approaches. Although several GWAS studies have identified 120 loci associated with blood pressure regulation, these explain only a tiny fraction of the phenotypic variants of blood pressure, thus resulting in a considerable proportion of missing heritability (Williams et al. 2018; Warren et al. 2017).

Additionally, hypertension is a highly heterogeneous disorder, and most individual biomarkers are only modestly associated with hypertension risk (Sesso et al. 2003; Vasan et al. 2004; Mandel et al. 2013; Yao et al. 2016), which makes them impractical for clinical use. Owing to their intracellular signaling, several circulating molecules are mechanistically correlated with each other. Hence, monitoring multiple biomarkers and targeting the pathway in which they are involved could provide the chance to develop disease-modifying therapy and reduce the incidence of cardiovascular diseases. Although not recommended in current guidelines (Williams et al. 2018), increasing evidence strongly suggests the potential use for a biomarker-based strategy for the stratification and clinical management of hypertension (Pandey et al. 2019).

In this study, the strong mechanism provided and the observation that sortilin, ASM, S1P and sNOX2-dp levels increase was more pronounced in uncontrolled

hypertensives, add new clinical perspectives for future development of multiple biomarker-based approach, aiming at improving the ability to predict and monitor the progression of hypertension.

A better understanding of the molecular mechanisms involved in the pathogenesis of hypertension will allow to predict the lack of response to standard pharmacological treatment and prevent the onset of polypharmacy side effects that also compromise the patient's health status favoring the development of chronic complex conditions.

6. MATERIALS AND METHODS

6.1 Reagents

To characterize intracellular signaling, human umbilical vein endothelial cells (HUVECs) or mesenteric arteries were pre-treated with the following before data were obtained: Tempol 100 μ M (Sigma-Aldrich) for 1 hour; K145 (Sigma-Aldrich, #SML1003) 1.5 μ M for 1 hour; (2R, 3S, 4E)-N-methyl-5-(4'-pentylphenyl)-2-aminopent-4-ene-1,3-diol (SK1-I) 5 μ M (Enzo, #BML-EI411) for 1 hour; W146 100nM (Sigma-Aldrich, #W1020) for 30 minutes; N-(4-chlorophenyl)-3,3-dimethyl-2-oxobutanimidic acid, 2-(4-chlorophenyl)hydrazide (TY52156) 5 μ M (Cayman Chemical, #19119) for 30 minutes; NSC23766 (Tocris #2161) 30 μ M was co-incubated with sortilin for 1 h; ML171 (Tocris, #4653) 1.5 μ M for 30 minutes; GSK2795039 (MCE #HY-18950) for 30 minutes; gp91 ds-tat (ANASPEC #AS-63818) 50 μ M for 30 minutes; PEG-SOD (Sigma #S9549) 200 U/mL for 1 hour. Plasma levels of sortilin were measured using ELISA Kit (Elabscience; #E-EL-H5414) following the manufacturer's protocol. Acidic sphingomyelinase activity was determined in human plasma samples and cell lysates by Acidic Sphingomyelinase Assay Kit (Abcam, #ab190554).

6.2 Mice

All experiments were conducted on 8-week-old male mice. We used C57BL/6J as wild-type (WT), and gp91^{phox}^{-/-} and S1P3^{-/-} mice (both in a C57BL/6J background) on a regular diet. All animals were randomly divided into control and sortilin-treated groups and had free access to standard mice chow and water. Mice were housed in groups (4–6 mice per cage) in a specific pathogen-free controlled environment under a normal 12 h light-12 h dark cycle. Mouse studies were carried out in accordance with the Guide for the Care and Use of Laboratory Animals published by the US National Institutes of Health and were approved by the IRCCS INM Neuromed review board (n° 1070/2015 PR).

6.2.1 Vascular reactivity studies

Vascular reactivity studies were performed on second-order branches of the mesenteric artery. Quantification of vasomotor response, blood pressure, and molecular analyses were performed by a second individual who was blind to the genotype of the animal and/or the hypothesis that was being tested for each group. Briefly, vessels were isolated and dissected from fat and connective tissue in ice-cold Krebs solution and gassed with 95% O₂ and 5% CO₂. Subsequently, arteries were mounted on a pressure myograph in organ chambers with Krebs solution and treated with increasing concentrations of U46619 (10⁻⁹ to 10⁻⁶ M) in order to obtain a similar level of pre-contraction in each ring (80% of initial KCl-induced contraction). Caution was taken to avoid damage to the endothelium; functional

integrity of the endothelium was confirmed by the vasodilation response to acetylcholine (10^{-9} to 10^{-6} M). Vasorelaxation was expressed as percent reduction of U46619-induced contraction.

6.2.2 Gene silencing

Second-order branches of the mesenteric arterial tree were removed from C57BL/6 mice and transfected with PKC ϵ siRNA (Santa Cruz, #sc-36250); AS β siRNA (Santa Cruz, #sc-41651); SphK1 siRNA (Santa Cruz, #sc-45446); SphK2 siRNA (Santa Cruz, #sc-39226) or aCDase siRNA (Santa Cruz, #sc-140807) and their relative Scramble vectors for 6 hours. Vessels were placed in a Mulvany pressure system filled with Krebs solution supplemented with 20 μ g of siRNA vector. All vessels were perfused at 100 mmHg for 1 h and then at 60 mmHg for 5 h.

Endothelium-dependent and independent relaxation were assessed by measuring the dilatory responses of mesenteric arteries to cumulative concentrations of acetylcholine (from 10^{-9} M to 10^{-5} M) or nitroglycerin (from 10^{-9} M to 10^{-5} M) in vessels pre-contracted with U46619 at a dose necessary to obtain a similar level of pre-contraction (80% of initial KCl-evoked contraction) in each vessel. Caution was taken to avoid endothelial damage. The corresponding values are reported as a percentage of lumen diameter change after exposure to the substance. Responses were tested before and after transfection with described plasmids, in presence or absence of sortilin (2,5 ng/mL for 1 h).

6.2.3 Nitric oxide detection

NO production in response to different stimuli as reported in figure legends was assessed and imaged using 4-amino-5-Methylamino-2',7-Difluorofluorescein Diacetate (DAF-FM) (Invitrogen, #D-23842). Briefly, isolated mesenteric arteries were embedded in a freezing medium to obtain transverse sections. Cryostat frozen cross sections (10 μm) were incubated with DAF-FM (12.5 μM) diluted in phosphate buffer with 0.4 mM CaCl_2 and incubated in a light protected humidified chamber at 37 $^\circ\text{C}$ for 1 h. Slices were washed in PBS and then mounted on a glass slide for fluorescence microscopy. Images were acquired by fluorescence microscopy (Zeiss, Jena, Germany) and then analyzed using ImageJ software. The fluorescence intensity was calculated using integrated density (area x mean fluorescence) by measuring the mean optical fluorescence density.

To evaluate the nitrite level in organ bath solution from pressure myograph, we used 280i Nitric Oxide Analyzer (Sievers Instruments). Briefly, prior to analysis, a mixture of glacial acetic acid and 1.0 mL of 0.5 M ascorbic acid was added to the purge bath to generate a calibration curve for nitrite. This method is specific for nitrite since the reaction mixture does not release NO from any other NO_x metabolites. All samples were thawed in the dark just prior to analysis and kept on ice until injected. Every four injections, the reagents of the purge bath were changed. The concentration of nitrite in the samples was determined using the

purge system of a Sievers Instruments model 280i nitric oxide analyzer. The specificity for both NO detection methods was confirmed by using the eNOS inhibitor N(ω)-nitro-L-arginine methyl ester L-NAME on mesenteric arteries (300 μ mol/L for 30 minutes Sigma-Aldrich; #N5751).

6.2.4 Evans blue Dye

The functional integrity of the endothelial layer of mesenteric arteries was also assessed 14 days after treatment with or sortilin using Evans Blue Dye (Sigma-Aldrich). Briefly, 2% Evans blue dye solution diluted in saline was injected into the tail vein 30 minutes before euthanasia, followed by PBS perfusion. Images were captured with an LSM 510 microscope (Carl Zeiss MicroImaging).

6.2.5 In vivo sortilin administration

To assess the acute effect of sortilin on blood pressure control, mice received a single intraperitoneal injection of sortilin (40 ng/mL, i.p.), and blood pressure was measured every hour until 6 hours after injection. In another set of experiments, WT mice were injected with TY52156 (S1P3 antagonist, 3 mg/kg i.p.) or vehicle (DMSO, 0.05%) after 2 hours from sortilin administration and blood pressure was measured at the same time points. For chronic sortilin infusion, mice were treated with sortilin (40 ng/mL/day) or the vehicle alone (saline solution 0.9%) via subcutaneous osmotic mini pumps (model ALZET 1002). For osmotic pumps implantation, mice were anesthetized with 1.5-2% isoflurane. A 1-cm incision was

made in the right dorsum. Then, the pump containing recombinant sortilin protein or vehicle (saline solution 0.9%) was inserted in 8 weeks-old WT, S1P3^{-/-}, and gp91^{phox^{-/-}} male mice and the wound was closed with sutures. After implantation, mice were injected with carprofen (5 mg/kg, s.c.) as postoperative analgesic. Blood pressure was measured every other day from day 0 to day 14 of vehicle or sortilin infusion. At the end of treatment, animals were sacrificed under terminal isoflurane anesthesia.

6.2.6 Blood pressure measurements

Blood pressure was measured in conscious mice by tail-cuff system (BP-2000, VisiTech Systems, Apex, NC). Briefly, animals were placed in a plastic chamber maintained at 34°C, and a cuff with a pneumatic pulse sensor was attached to the tail. For tail-cuff system, mice were subjected at least to seven days of training, and basal blood pressure levels were recorded as the average of values determined on at least three days.

6.3 Cell Culture

Commercially available HUVECs were obtained from ATCC. Cells were cultured in Vascular Cell Basal Medium supplemented with Endothelial Cell Growth Kit before experiments were performed. Cells were maintained at 37°C and 5% CO₂ in a humidified incubator. Before experiments, HUVECs were seeded in 24-well plates, 60 mm or 100mm dishes and grown until 80% confluency.

6.4 Measurement of ROS production

6.4.1 Sensitive fluorescent indicator dihydroethidium

Dihydroethidium (DHE) was used to evaluate the levels of oxidative stress in mesenteric arteries and in HUVECs. Briefly, vessels were immediately snap-frozen with OCT embedding compound in isopentane prechilled with liquid nitrogen and transverse sections (7 or 10 μm) were produced using a cryostat (Leica CM1250). Sections were then incubated with 2 or 100 $\mu\text{mol/L}$ DHE (Sigma-Aldrich, #309800) for 20 minutes at 37°C in a humidified chamber protected from light and then observed under a fluorescence microscope (Zeiss, Oberkochen, Germany). The fluorescence intensity was quantified as arbitrary units using Image J software. To quantify O_2^- in HUVECs, we measured DHE fluorescence using a microplate reader. At the end of the treatments, cells were incubated with a final DHE concentration of 5 μM for 30 min. The resulting mixtures were harvested in acetonitrile (0.2 mL/well), sonicated (10 s), and centrifuged (13,000 g for 5 min at 4°C). The supernatant fraction was air-dried, reconstituted in PBS and fluorescence was determined, in duplicate, using a microplate reader at excitation and emission wavelengths of 490 and 570 nm, respectively.

6.4.2 Evaluation of NADPH-Mediated O_2^- Production

NADPH oxidase-mediated superoxide radical (O_2^-) production was evaluated by using the lucigenin-enhanced chemiluminescence assay. HUVECs were cultured in

60 mm dishes. After reaching confluence, cells were washed with PBS, detached using 0.25% trypsin/EDTA (1 mmol/l) and resuspended in modified HEPES buffer containing (mmol/l) NaCl 140, KCl 5, MgCl₂ 0.8, CaCl₂ 1.8, Na₂HPO₄ 1, HEPES 25 and 1% glucose, pH 7. Subsequently, cells were homogenated, and a total of 100 µg of extract was distributed on a 96-well microplate. Vessels were incubated in Krebs buffer and equilibrated for 30 minutes at 37°C.

Vessels were homogenized in a buffer containing protease inhibitors (mmol/L: 20 monobasic potassium phosphate, 1 EGTA, 0.01 aprotinin, 0.01 leupeptin, 0.01 pepstatin, 0.5 phenylmethylsulfonyl fluoride, pH 7.0). Protein content was measured in an aliquot of the homogenate by Bradford method. The reaction was started by the addition of NADPH (0.1 mmol/l) and lucigenin (5 µmol/l) to each well. The chemiluminescence was measured using Tecan Infinite Pro M200 multimode microplate at 37°C.

6.5 Flow cytometry

HUVEC single-cell suspensions were stained with mouse anti-Human S1P3/EDG-3 PE-conjugated Antibody (Monoclonal Mouse IgG2A Clone #776808; R&D Systems). After 30 min incubation at 4°C in the dark, cells were washed and resuspended in staining buffer (PBS 2% FBS) for the flow cytometry acquisition and analysis using FACS Verse Flow Cytometer (BD Biosciences).

6.6 qRT-PCR analysis

Total RNA was extracted with TRI reagent (Sigma-Aldrich), quantified by NanoDrop™ 1000 spectrophotometer (Thermo Fisher Scientific), treated with DNase I (Invitrogen) and reverse transcribed using a SuperScript™ VILO™ Master Mix (Invitrogen, #11755500). Specific cDNAs were amplified and analyzed using a 7500 Real-Time PCR System (Applied Biosciences). Primer sequences (forward and reverse, respectively) were as follows: *S1P3*, 5'-TGATTGTGGTGAGCGTGTTC-3', 5'-GGCCACATCAATGAGGAAGAG-3', (Yoon et al. 2008). Quantification was performed using Δ CT calculation.

6.7 Immunofluorescence and confocal fluorescence imaging

Confluent HUVECs seeded onto 12 mm glass coverslips were pre-treated with TY-52156 (30 min) inhibitor or vehicle (DMSO 0.02%) prior to sortilin, and fixed with 4% paraformaldehyde in 0.1 M PBS buffer for 15 min at room temperature. Cells were permeabilized using PBS containing 0.005% saponin for 30 min and incubated overnight at 4°C with IgG primary rabbit polyclonal anti-Rac1 (Abcam, Anti-Rac1 antibody #ab97732), followed by a 1-hour incubation with the secondary antibodies Alexa Fluor 488 conjugated anti-rabbit IgG (Invitrogen, #A11008) and DyLight 549 conjugated anti-rabbit IgG (Vector Laboratories, #DI-1549).

Images were acquired using a confocal laser-scanning fluorescence microscope TCS SP5 (Leica Microsystems). Nuclei were stained with DAPI.

6.8 Western blot

For total protein extraction, pooled mesenteric arteries or cells were lysed in a buffer containing 150 mmol/L NaCl, 50 mmol/L Tris-HCl (pH 8.5), 2 mmol/L EDTA, 1% v/v NP-40, 0.5 % w/v deoxycholate, 10 mmol/L NaF, 10 mM sodium pyrophosphate, 2 mmol/L PMSF, 2 g/ml leupeptin, and 2 g/ml aprotinin (pH 7.4). Lysates were then centrifuged at 38000 x g for 30 min at 4°C to collect the supernatant. Protein concentration was measured using a dye-binding protein assay kit (Bio-Rad) and reading at the spectrophotometer at a wavelength of 595 nm. Immunoblotting was performed using the following antibodies: anti-phospho-eNOS serine 1177 (Enzo Life Sciences, ALX-804-396-C100); anti-phospho-eNOS-Thr495 (Cell Signaling Technology, #9574); anti-eNOS (Cell Signaling, #9570); anti- β -Actin (Abcam, mAb #ab8226); anti-phospho-Protein-Tyrosine Kinase 2-Beta Phospho-Tyr579 (PYK2 pY579) (Elabscience, #E-AB-21240); anti-phospho-PKC ϵ Ser729 (Biorbyt, #orb315664); anti-PKC alpha (phospho T497) antibody [EP2608Y] (Abcam, #ab76016); anti-PKC-PAN (Sigma-Aldrich, #SAB4502356); anti-ASMase (SMPD1; Biorbyt, #ORB214591); anti-S1P1 (Immunological Sciences, #AB-83739); anti-S1P3 (Elabscience, #E-AB-31267); anti-gp91phox (54.1) (Santa Cruz, #sc-130543); anti-SphK1 (G-11) (Santa Cruz, #sc-365401); anti-SphK2 (MyBioSource, #MBS2518663); anti-aCDase (ASAH1; MyBioSource, #MBS1492517), anti-Active Rac1 (Rac1-GTP) (Neweast bioscience #26903). Secondary antibodies were purchased from Amersham Life Sciences (GE Healthcare). Bands were visualized

with enhanced chemiluminescence (ECL, Amersham Life Sciences), according to the manufacturer's instructions. Immunoblotting data were analyzed using ImageJ software (developed by Wayne Rasband, NIH, USA) to determine density of the bands.

6.9 Human subjects

All human data was collected in accordance with the Declaration of Helsinki and with local Ethics Committee approval. Individuals from two prospective Italian studies were included: The Campania Salute Network Study (University of Naples Federico II; permit number: 16/14) and the Moli-Sani Study (Catholic University of Rome, Italy; permit number: P99, A.931/03-138-04/C.E./2004). Written informed consent was obtained from all included participants.

Campania Salute Network. 71 patients with hypertension (defined as DBP \geq 90 mmHg and SBP \geq 140 mmHg or on the basis of use of anti-hypertensive medication) and 71 healthy donor control subjects belonging to the Campania Salute Network Registry, were studied. Campania Salute is an open registry collecting information from a network of general practitioners and community hospitals networked with the Hypertension Center of Federico II University Hospital, Naples. The database generation of the Campania Salute Network was approved by the Federico II University Hospital Ethic Committee. All patients had

no history of previous cardiovascular diseases, symptomatic heart failure, ischemic heart disease, atrial fibrillation, stroke or cognitive dysfunction.

Moli-Sani Study. We collected a total of 289 plasma samples from the biodata bank of the Moli-Sani Study, a prospective cohort study established in 2005 to 2010 with an enrollment of 24,325 men and women (≥ 35 years of age) randomly recruited from the general population of Molise, a southern Mediterranean region in Italy (Di Castelnuovo et al. 2012). Data are accessible upon written request to the Moli-Sani Study PI, Prof. Licia Iacoviello. 19 hemolyzed samples were excluded from the analysis. A total of 270 patients were stratified in normotensives (N=89), and in controlled (N=91) or uncontrolled hypertensive subjects (N=90), strictly matched and with no previous history of cardiovascular diseases. Hypertension was defined as controlled (SBP was < 140 and DBP < 90 mmHg with treatment), and uncontrolled (SBP was ≥ 140 and DBP ≥ 90 mmHg with treatment).

All patients included in this study were not on statin therapy, which is known to influence the circulating sortilin level (Nozue et al. 2016).

6.9.1 Evaluation of Human Endothelial Function by endoPAT

Endothelial function was evaluated in patients from the Campania Salute Network project using the EndoPAT 2000 device (Itamar Medical Ltd., Caesarea, Israel) for the determination of the reactive hyperemia index (RHI). Briefly, measurements were performed according to the manufacturer's instructions and were calculated

using a computerized automated algorithm (software version 3.1.2) provided with the device. Briefly, subjects were in supine position for a minimum of 15 min before measurements in a quiet, temperature-controlled (21–24°C) room with dimmed lights. The subjects were asked to remain as still as possible and silent during the entire measurement period. Each recording consisted of 5 min of baseline measurement, 5 min of occlusion measurement, and 5 min of post-occlusion measurement (hyperemic period). Occlusion of the brachial artery was performed on the non-dominant, upper arm. The occlusion pressure was at least 60 mmHg above the systolic blood pressure (minimally 200 mmHg, and maximally 300 mmHg).

6.9.2 Soluble NOX2-derived peptide ELISA detection.

NOX2 activation was measured in human plasma as soluble NOX2-derived peptide (sNOX2-dp) with an ELISA method. Briefly, the peptide is recognized by binding to a specific monoclonal antibody against the amino acid sequence (224-268), extra membrane portion of NOX2, which was released following platelet activation.

The enzyme activity is measured spectrophotometrically by the increased absorbency at 450 nm. Since the increase in absorbency is directly proportional to the amount of sNOX2-dp of the unknown sample, the latter can be derived by interpolation from a reference curve generated in the same assay with reference

standards of known concentrations of sNOX2-dp (0-200 pg/ml). Values were expressed as pg/ml; intra-assay and inter-assay coefficients of variation were 8.95% and 9.01%, respectively.

6.10 Sphingolipid analysis by LC-MS/MS

Confluent HUVECs were incubated with recombinant sortilin (2.5 ng/mL, 1 h) diluted in Vascular Cell Basal Medium and supplemented with Endothelial Cell Growth Kit. The culture medium and cell lysates were analyzed for extracellular S1P and intracellular ceramide content, respectively. All solvent and additives were LCMS grade and purchased from Sigma-Aldrich (Milan, Italy). Standard of S1P, Ceramides C16, C18, C24:1 and deuterated Ceramide mix were purchased by Avanti Polar Lipids (Alabaster, AL, U.S.A). For the extraction of sphingolipids, human plasma (20 μ l) were diluted to 400 μ L with Milli-Q water, and 3 microliters of the internal standard were added, following samples were extracted by addition of 400 μ L of isopropanol/ethyl acetate 18/85 (v/v), vortexed for 20 sec and centrifuged for 5 minutes at 14580 rpm. The upper organic phase was collected, while the aqueous phase was acidified with 20 μ L of formic acid and re-extracted with 400 μ L of fresh isopropanol/ethyl acetate 18/85 (v/v%). The obtained solution was vortexed and centrifuged. The supernatants were pooled and dried under a gentle stream of nitrogen.

For sphingolipid extraction, cell media (500 μ L) were diluted with 1mL isopropanol/ethyl acetate 18/85 (v/v%) and processed as described above. Samples were re-solubilized with 150 μ L of Methanol, 1 mM HCOONH₄ plus 0.2% HCOOH (v/v). UHPLC-MS/MS analysis was carried out with a Shimadzu Nexera (Shimadzu, Milan, Italy) coupled online to a triple quadrupole LCMS 8050 (Shimadzu, Kyoto, Japan) by an ESI source.

UHPLC-MS/MS conditions. The separation was performed on a Kinetex EVO C18 150 mm x 2.1 mm, 2.6 μ m (Phenomenex, Bologna, Italy), at a flow rate of 0.5 mL/min, employing as mobile phase A) ACN/H₂O: 60/40 10 mM HCOONH₄ plus 0.1% HCOOH (v/v%), and B) Isopropanol/ACN 90/10 plus 0.1% HCOOH (v/v%) with the following gradient: 0 min, 5% B, 0-2.50 min, 50% B, 2.51-7 min 50-99% B, isocratic for 2.50 min. Returning to 5% in 4 min. 5 microliters were injected. The ESI was operated in positive ionization. MS source parameters were: Interface temperature 300°C, Desolvation line temperature 250°C, Heat Block temperature 400°C; nebulizing gas, drying gas, and heating gas were set respectively to 3, 10, 10 L/min. MS/MS analysis of sphingolipids was performed in multiple reaction monitoring (MRM). The SRM transition of non-available ceramides was in silico optimized using the Lipid Creator tool in the freely available Skyline open source (Peng et al. 2020).

6.11 Statistics

Results are expressed as mean \pm SD. The Shapiro-Wilk test was used to evaluate the normality of distribution of investigated parameters. Two-sided unpaired Student's *t*-test was performed for comparisons between two independent groups. One-way ANOVA (with Bonferroni's correction) or, when normality test failed, non-parametric Kruskal-Wallis test (with Dunn's multiple comparison) was used for comparisons of multiple means. Two-way ANOVA (with Bonferroni's correction) was used for comparisons of concentration-response curves. Two-way ANOVA for repeated measurements (with Bonferroni's correction for comparison of multiple means) was used to calculate statistical significance of blood pressure measurements in mice. Fisher's exact test or, where appropriate, Chi-Square test were used for comparison of categorical data between study subjects. Pearson's correlation analysis was used to measure the degree of correlation between two variables. The gradient of linear model and its 95% confidence interval has been calculated to verify whether there was a statistically significant difference between the two variables. A *P* value less than 0.05 was considered significant. Statistical analysis was performed with GraphPad Prism software (version 8.0, GraphPad Software, San Diego, CA), MATLAB software (version R2019b, The Mathwork Inc) and the MES toolbox in MATLAB, Harald Hentschke, 2020 hhentschke/measures-of-effect-size-toolbox (<https://www.github.com/hhentschke/measures-of-effect-size-toolbox>), GitHub.

7. REFERENCES

- Alexander, M. Y., M. J. Brosnan, C. A. Hamilton, et al. 1999. 'Gene transfer of endothelial nitric oxide synthase improves nitric oxide-dependent endothelial function in a hypertensive rat model', *Cardiovasc Res*, 43: 798-807.
- Bao, J. X., S. Jin, F. Zhang, et al. 2010. 'Activation of membrane NADPH oxidase associated with lysosome-targeted acid sphingomyelinase in coronary endothelial cells', *Antioxid Redox Signal*, 12: 703-12.
- Bayer, A. L., M. C. Heidkamp, A. L. Howes, et al. 2003. 'Protein kinase C epsilon-dependent activation of proline-rich tyrosine kinase 2 in neonatal rat ventricular myocytes', *J Mol Cell Cardiol*, 35: 1121-33.
- Bedard, K., and K. H. Krause. 2007. 'The NOX family of ROS-generating NADPH oxidases: physiology and pathophysiology', *Physiol Rev*, 87: 245-313.
- Biscetti, F., N. Bonadia, F. Santini, et al. 2019. 'Sortilin levels are associated with peripheral arterial disease in type 2 diabetic subjects', *Cardiovasc Diabetol*, 18: 5.
- Blondeau, N., S. Beraud-Dufour, P. Lebrun, et al. 2018. 'Sortilin in Glucose Homeostasis: From Accessory Protein to Key Player?', *Front Pharmacol*, 9: 1561.
- Cantalupo, A., A. Gargiulo, E. Dautaj, et al. 2017. 'S1PR1 (Sphingosine-1-Phosphate Receptor 1) Signaling Regulates Blood Flow and Pressure', *Hypertension*, 70: 426-34.
- Carrizzo, A., O. Moltedo, A. Damato, et al. 2020. 'New Nutraceutical Combination Reduces Blood Pressure and Improves Exercise Capacity in Hypertensive Patients Via a Nitric Oxide-Dependent Mechanism', *J Am Heart Assoc*, 9: e014923.
- Castro, B. M., M. Prieto, and L. C. Silva. 2014. 'Ceramide: a simple sphingolipid with unique biophysical properties', *Prog Lipid Res*, 54: 53-67.
- Chen, C., J. Li, D. J. Matye, et al. 2019. 'Hepatocyte sortilin 1 knockout and treatment with a sortilin 1 inhibitor reduced plasma cholesterol in Western diet-fed mice', *J Lipid Res*, 60: 539-49.
- Cheng, H. S., R. Besla, A. Li, et al. 2017. 'Paradoxical Suppression of Atherosclerosis in the Absence of microRNA-146a', *Circ Res*, 121: 354-67.
- Cheng, J. J., Y. J. Chao, and D. L. Wang. 2002. 'Cyclic strain activates redox-sensitive proline-rich tyrosine kinase 2 (PYK2) in endothelial cells', *J Biol Chem*, 277: 48152-7.
- Chu, Y., S. Iida, D. D. Lund, et al. 2003. 'Gene transfer of extracellular superoxide dismutase reduces arterial pressure in spontaneously hypertensive rats: role of heparin-binding domain', *Circ Res*, 92: 461-8.
- Chun, J., T. Hla, K. R. Lynch, et al. 2010. 'International Union of Basic and Clinical Pharmacology. LXXVIII. Lysophospholipid receptor nomenclature', *Pharmacol Rev*, 62: 579-87.
- Dandona, P., R. Karne, H. Ghanim, et al. 2000. 'Carvedilol inhibits reactive oxygen species generation by leukocytes and oxidative damage to amino acids', *Circulation*, 101: 122-4.
- Deutschman, D. H., J. S. Carstens, R. L. Klepper, et al. 2003. 'Predicting obstructive coronary artery disease with serum sphingosine-1-phosphate', *Am Heart J*, 146: 62-8.

- Di Castelnuovo, A., S. Costanzo, M. Persichillo, et al. 2012. 'Distribution of short and lifetime risks for cardiovascular disease in Italians', *Eur J Prev Cardiol*, 19: 723-30.
- Di Pietro, P., A. Carrizzo, E. Sommella, et al. 2022. 'Targeting the ASMAse/S1P pathway protects from sortilin-evoked vascular damage in hypertension', *J Clin Invest*, 132.
- Dikalova, A., R. Clempus, B. Lassegue, et al. 2005. 'Nox1 overexpression potentiates angiotensin II-induced hypertension and vascular smooth muscle hypertrophy in transgenic mice', *Circulation*, 112: 2668-76.
- Drummond, G. R., S. Selemidis, K. K. Griendling, et al. 2011. 'Combating oxidative stress in vascular disease: NADPH oxidases as therapeutic targets', *Nat Rev Drug Discov*, 10: 453-71.
- Goettsch, C., J. D. Hutcheson, M. Aikawa, et al. 2016. 'Sortilin mediates vascular calcification via its recruitment into extracellular vesicles', *J Clin Invest*, 126: 1323-36.
- Goettsch, C., H. Iwata, J. D. Hutcheson, et al. 2017. 'Serum Sortilin Associates With Aortic Calcification and Cardiovascular Risk in Men', *Arterioscler Thromb Vasc Biol*, 37: 1005-11.
- Goettsch, C., M. Kjolby, and E. Aikawa. 2018. 'Sortilin and Its Multiple Roles in Cardiovascular and Metabolic Diseases', *Arterioscler Thromb Vasc Biol*, 38: 19-25.
- Griendling, K. K., L. L. Camargo, F. J. Rios, et al. 2021. 'Oxidative Stress and Hypertension', *Circ Res*, 128: 993-1020.
- Hassanain, H. H., D. Gregg, M. L. Marcelo, et al. 2007. 'Hypertension caused by transgenic overexpression of Rac1', *Antioxid Redox Signal*, 9: 91-100.
- Higashi, Y., Y. Kihara, and K. Noma. 2012. 'Endothelial dysfunction and hypertension in aging', *Hypertens Res*, 35: 1039-47.
- Inoguchi, T., T. Sonta, H. Tsubouchi, et al. 2003. 'Protein kinase C-dependent increase in reactive oxygen species (ROS) production in vascular tissues of diabetes: role of vascular NAD(P)H oxidase', *J Am Soc Nephrol*, 14: S227-32.
- Jin, S., F. Yi, F. Zhang, et al. 2008. 'Lysosomal targeting and trafficking of acid sphingomyelinase to lipid raft platforms in coronary endothelial cells', *Arterioscler Thromb Vasc Biol*, 28: 2056-62.
- Jones, G. T., M. J. Bown, S. Gretarsdottir, et al. 2013. 'A sequence variant associated with sortilin-1 (SORT1) on 1p13.3 is independently associated with abdominal aortic aneurysm', *Hum Mol Genet*, 22: 2941-7.
- Jung, O., S. L. Marklund, H. Geiger, et al. 2003. 'Extracellular superoxide dismutase is a major determinant of nitric oxide bioavailability: in vivo and ex vivo evidence from ecSOD-deficient mice', *Circ Res*, 93: 622-9.
- Jung, O., J. G. Schreiber, H. Geiger, et al. 2004. 'gp91phox-containing NADPH oxidase mediates endothelial dysfunction in renovascular hypertension', *Circulation*, 109: 1795-801.
- Kathiresan, S., A. K. Manning, S. Demissie, et al. 2007. 'A genome-wide association study for blood lipid phenotypes in the Framingham Heart Study', *BMC Med Genet*, 8 Suppl 1: S17.
- Kathiresan, S., O. Melander, C. Guiducci, et al. 2008. 'Six new loci associated with blood low-density lipoprotein cholesterol, high-density lipoprotein cholesterol or triglycerides in humans', *Nat Genet*, 40: 189-97.
- Katusic, Z. S., and S. A. Austin. 2014. 'Endothelial nitric oxide: protector of a healthy mind', *Eur Heart J*, 35: 888-94.

- Khan, B. V., S. Navalkar, Q. A. Khan, et al. 2001. 'Irbesartan, an angiotensin type 1 receptor inhibitor, regulates the vascular oxidative state in patients with coronary artery disease', *J Am Coll Cardiol*, 38: 1662-7.
- Kjolby, M., O. M. Andersen, T. Breiderhoff, et al. 2010. 'Sort1, encoded by the cardiovascular risk locus 1p13.3, is a regulator of hepatic lipoprotein export', *Cell Metab*, 12: 213-23.
- Kjolby, M., M. S. Nielsen, and C. M. Petersen. 2015. 'Sortilin, encoded by the cardiovascular risk gene SORT1, and its suggested functions in cardiovascular disease', *Curr Atheroscler Rep*, 17: 496.
- Kornhuber, J., P. Tripal, M. Reichel, et al. 2010. 'Functional Inhibitors of Acid Sphingomyelinase (FIASMs): a novel pharmacological group of drugs with broad clinical applications', *Cell Physiol Biochem*, 26: 9-20.
- Lassegue, B., and K. K. Griendling. 2010. 'NADPH oxidases: functions and pathologies in the vasculature', *Arterioscler Thromb Vasc Biol*, 30: 653-61.
- Lefrancois, S., J. Zeng, A. J. Hassan, et al. 2003. 'The lysosomal trafficking of sphingolipid activator proteins (SAPs) is mediated by sortilin', *EMBO J*, 22: 6430-7.
- Li, J., D. J. Matye, and T. Li. 2015. 'Insulin resistance induces posttranslational hepatic sortilin 1 degradation in mice', *J Biol Chem*, 290: 11526-36.
- Li, J., Y. Wang, D. J. Matye, et al. 2017. 'Sortilin 1 Modulates Hepatic Cholesterol Lipotoxicity in Mice via Functional Interaction with Liver Carboxylesterase 1', *J Biol Chem*, 292: 146-60.
- Lin, C. C., C. C. Yang, R. L. Cho, et al. 2016. 'Sphingosine 1-Phosphate-Induced ICAM-1 Expression via NADPH Oxidase/ROS-Dependent NF-kappaB Cascade on Human Pulmonary Alveolar Epithelial Cells', *Front Pharmacol*, 7: 80.
- Linsel-Nitschke, P., J. Heeren, Z. Aherrahrou, et al. 2010. 'Genetic variation at chromosome 1p13.3 affects sortilin mRNA expression, cellular LDL-uptake and serum LDL levels which translates to the risk of coronary artery disease', *Atherosclerosis*, 208: 183-9.
- Machida, T., R. Matamura, K. Iizuka, et al. 2016. 'Cellular function and signaling pathways of vascular smooth muscle cells modulated by sphingosine 1-phosphate', *J Pharmacol Sci*, 132: 211-17.
- Mandel, E. I., J. P. Forman, G. C. Curhan, et al. 2013. 'Plasma bicarbonate and odds of incident hypertension', *Am J Hypertens*, 26: 1405-12.
- Matsuno, K., H. Yamada, K. Iwata, et al. 2005. 'Nox1 is involved in angiotensin II-mediated hypertension: a study in Nox1-deficient mice', *Circulation*, 112: 2677-85.
- Miller, W. H., M. J. Brosnan, D. Graham, et al. 2005. 'Targeting endothelial cells with adenovirus expressing nitric oxide synthase prevents elevation of blood pressure in stroke-prone spontaneously hypertensive rats', *Mol Ther*, 12: 321-7.
- Mochly-Rosen, D., K. Das, and K. V. Grimes. 2012. 'Protein kinase C, an elusive therapeutic target?', *Nat Rev Drug Discov*, 11: 937-57.
- Morris, N. J., S. A. Ross, W. S. Lane, et al. 1998. 'Sortilin is the major 110-kDa protein in GLUT4 vesicles from adipocytes', *J Biol Chem*, 273: 3582-7.
- Mortensen, M. B., M. Kjolby, S. Gunnarsen, et al. 2014. 'Targeting sortilin in immune cells reduces proinflammatory cytokines and atherosclerosis', *J Clin Invest*, 124: 5317-22.

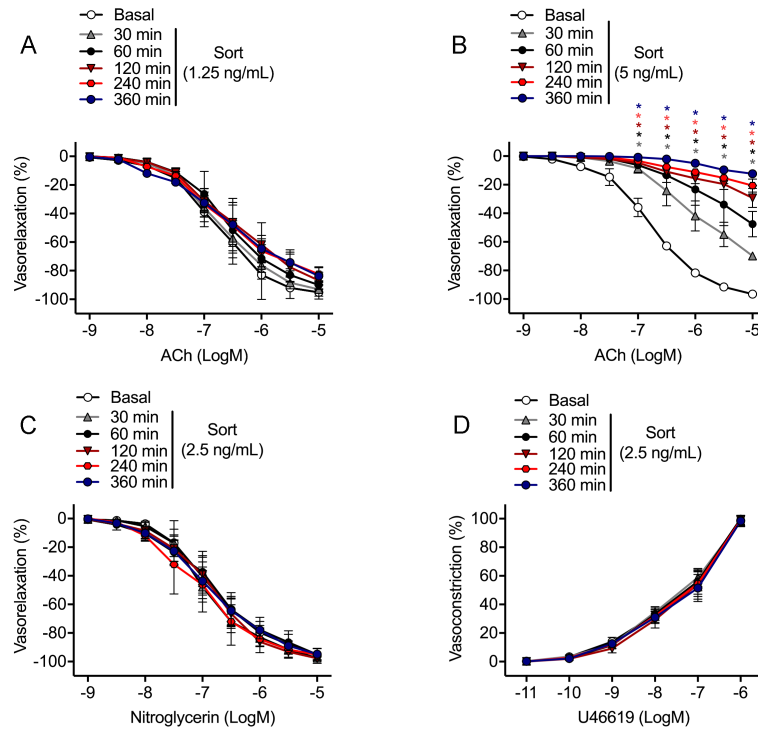
- Muendlein, A., S. Geller-Rhomberg, C. H. Saely, et al. 2009. 'Significant impact of chromosomal locus 1p13.3 on serum LDL cholesterol and on angiographically characterized coronary atherosclerosis', *Atherosclerosis*, 206: 494-9.
- Munck Petersen, C., M. S. Nielsen, C. Jacobsen, et al. 1999. 'Propeptide cleavage conditions sortilin/neurotensin receptor-3 for ligand binding', *EMBO J*, 18: 595-604.
- Musunuru, K., A. Strong, M. Frank-Kamenetsky, et al. 2010. 'From noncoding variant to phenotype via SORT1 at the 1p13 cholesterol locus', *Nature*, 466: 714-9.
- Myocardial Infarction Genetics, Consortium, S. Kathiresan, B. F. Voight, et al. 2009. 'Genome-wide association of early-onset myocardial infarction with single nucleotide polymorphisms and copy number variants', *Nat Genet*, 41: 334-41.
- Nabha, L., J. C. Garbern, C. L. Buller, et al. 2005. 'Vascular oxidative stress precedes high blood pressure in spontaneously hypertensive rats', *Clin Exp Hypertens*, 27: 71-82.
- Nofer, J. R., M. van der Giet, M. Tolle, et al. 2004. 'HDL induces NO-dependent vasorelaxation via the lysophospholipid receptor S1P3', *J Clin Invest*, 113: 569-81.
- Nozue, T., H. Hattori, K. Ogawa, et al. 2016. 'Effects of Statin Therapy on Plasma Proprotein Convertase Subtilisin/kexin Type 9 and Sortilin Levels in Statin-Naive Patients with Coronary Artery Disease', *J Atheroscler Thromb*, 23: 848-56.
- Nurnberg, S. T., H. Zhang, N. J. Hand, et al. 2016. 'From Loci to Biology: Functional Genomics of Genome-Wide Association for Coronary Disease', *Circ Res*, 118: 586-606.
- Oh, T. J., C. H. Ahn, B. R. Kim, et al. 2017. 'Circulating sortilin level as a potential biomarker for coronary atherosclerosis and diabetes mellitus', *Cardiovasc Diabetol*, 16: 92.
- Oparil, S., M. C. Acelajado, G. L. Bakris, et al. 2018. 'Hypertension', *Nat Rev Dis Primers*, 4: 18014.
- Ouyang, S., B. Jia, W. Xie, et al. 2020. 'Mechanism underlying the regulation of sortilin expression and its trafficking function', *J Cell Physiol*, 235: 8958-71.
- Pallesen, L. T., C. Gustafsen, J. F. Cramer, et al. 2020. 'PAK Kinases Target Sortilin and Modulate Its Sorting', *Mol Cell Biol*, 40.
- Pandey, A., K. V. Patel, W. Vongpatanasin, et al. 2019. 'Incorporation of Biomarkers Into Risk Assessment for Allocation of Antihypertensive Medication According to the 2017 ACC/AHA High Blood Pressure Guideline: A Pooled Cohort Analysis', *Circulation*, 140: 2076-88.
- Panza, J. A., C. E. Garcia, C. M. Kilcoyne, et al. 1995. 'Impaired endothelium-dependent vasodilation in patients with essential hypertension. Evidence that nitric oxide abnormality is not localized to a single signal transduction pathway', *Circulation*, 91: 1732-8.
- Park, J. B., F. Charbonneau, and E. L. Schiffrin. 2001. 'Correlation of endothelial function in large and small arteries in human essential hypertension', *J Hypertens*, 19: 415-20.
- Patel, K. M., A. Strong, J. Tohyama, et al. 2015. 'Macrophage sortilin promotes LDL uptake, foam cell formation, and atherosclerosis', *Circ Res*, 116: 789-96.
- Pavoine, C., and F. Pecker. 2009. 'Sphingomyelinases: their regulation and roles in cardiovascular pathophysiology', *Cardiovasc Res*, 82: 175-83.
- Pechanova, O., J. Zicha, S. Kojsova, et al. 2006. 'Effect of chronic N-acetylcysteine treatment on the development of spontaneous hypertension', *Clin Sci (Lond)*, 110: 235-42.

- Peng, B., D. Kopczynski, B. S. Pratt, et al. 2020. 'LipidCreator workbench to probe the lipidomic landscape', *Nat Commun*, 11: 2057.
- Petersen, C. M., M. S. Nielsen, A. Nykjaer, et al. 1997. 'Molecular identification of a novel candidate sorting receptor purified from human brain by receptor-associated protein affinity chromatography', *J Biol Chem*, 272: 3599-605.
- Polzin, A., C. Helten, L. Dannenberg, et al. 2021. 'Sphingosine-1-phosphate: A mediator of the ARB-MI paradox?', *Int J Cardiol*, 333: 40-42.
- Pontremoli, S., F. Salamino, B. Sparatore, et al. 1989. 'Enhanced activation of the respiratory burst oxidase in neutrophils from hypertensive patients', *Biochem Biophys Res Commun*, 158: 966-72.
- Poolman, T. M., P. A. Quinn, and L. Ng. 2013. 'Protein Kinase C Epsilon Contributes to NADPH Oxidase Activation in a Pre-Eclampsia Lymphoblast Cell Model', *Diseases*, 1: 1-17.
- Rajagopalan, S., S. Kurz, T. Munzel, et al. 1996. 'Angiotensin II-mediated hypertension in the rat increases vascular superoxide production via membrane NADH/NADPH oxidase activation. Contribution to alterations of vasomotor tone', *J Clin Invest*, 97: 1916-23.
- Sag, C. M., M. Schnelle, J. Zhang, et al. 2017. 'Distinct Regulatory Effects of Myeloid Cell and Endothelial Cell NADPH Oxidase 2 on Blood Pressure', *Circulation*, 135: 2163-77.
- Samani, N. J., J. Erdmann, A. S. Hall, et al. 2007. 'Genomewide association analysis of coronary artery disease', *N Engl J Med*, 357: 443-53.
- Sattler, K., I. Lehmann, M. Graler, et al. 2014. 'HDL-bound sphingosine 1-phosphate (S1P) predicts the severity of coronary artery atherosclerosis', *Cell Physiol Biochem*, 34: 172-84.
- Schulz, E., T. Gori, and T. Munzel. 2011. 'Oxidative stress and endothelial dysfunction in hypertension', *Hypertens Res*, 34: 665-73.
- Sedeek, M., R. L. Hebert, C. R. Kennedy, et al. 2009. 'Molecular mechanisms of hypertension: role of Nox family NADPH oxidases', *Curr Opin Nephrol Hypertens*, 18: 122-7.
- Sesso, H. D., J. E. Buring, N. Rifai, et al. 2003. 'C-reactive protein and the risk of developing hypertension', *JAMA*, 290: 2945-51.
- Shi, J., and K. V. Kandror. 2005. 'Sortilin is essential and sufficient for the formation of Glut4 storage vesicles in 3T3-L1 adipocytes', *Dev Cell*, 9: 99-108.
- Smith, J. G., K. Luk, C. A. Schulz, et al. 2014. 'Association of low-density lipoprotein cholesterol-related genetic variants with aortic valve calcium and incident aortic stenosis', *JAMA*, 312: 1764-71.
- Spiegel, S., and S. Milstien. 2003. 'Sphingosine-1-phosphate: an enigmatic signalling lipid', *Nat Rev Mol Cell Biol*, 4: 397-407.
- Spijkers, L. J., B. J. Janssen, J. Nelissen, et al. 2011. 'Antihypertensive treatment differentially affects vascular sphingolipid biology in spontaneously hypertensive rats', *PLoS One*, 6: e29222.
- Stocker, R., and J. F. Keaney, Jr. 2004. 'Role of oxidative modifications in atherosclerosis', *Physiol Rev*, 84: 1381-478.
- Strong, A., Q. Ding, A. C. Edmondson, et al. 2012. 'Hepatic sortilin regulates both apolipoprotein B secretion and LDL catabolism', *J Clin Invest*, 122: 2807-16.

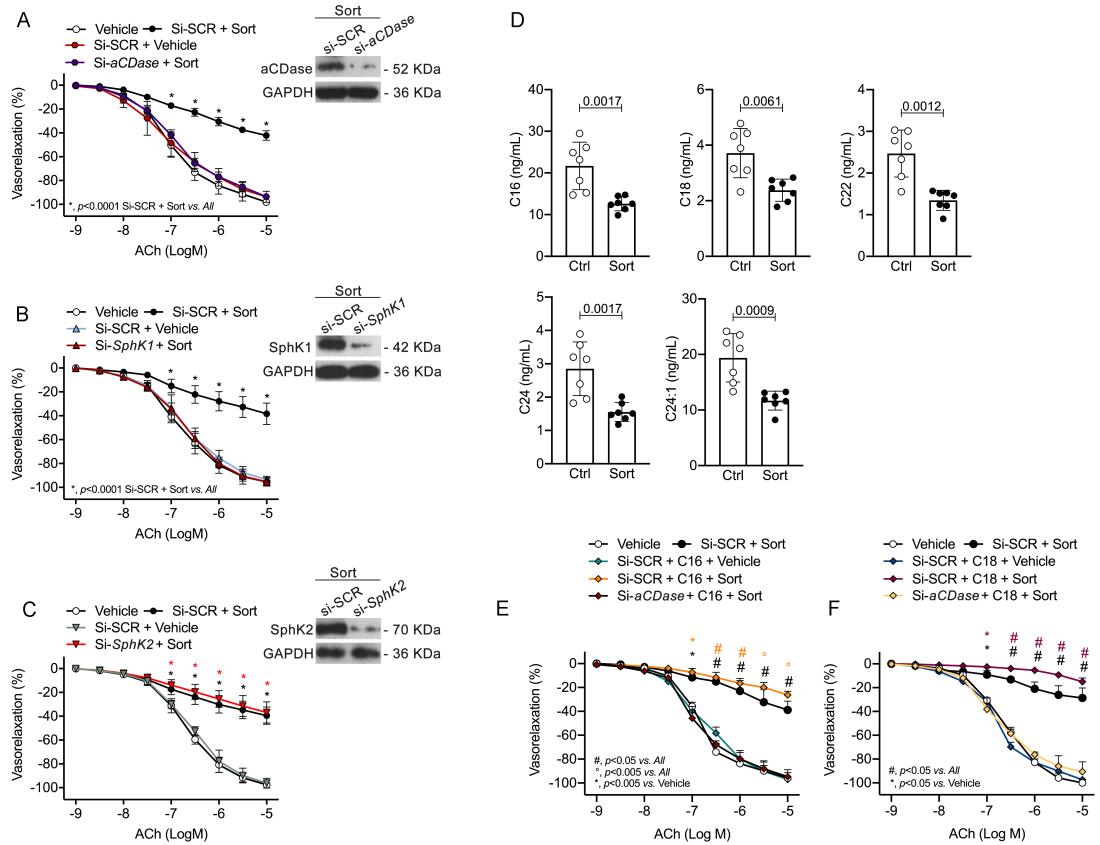
- Taddei, S., L. Ghiadoni, A. Viridis, et al. 2003. 'Mechanisms of endothelial dysfunction: clinical significance and preventive non-pharmacological therapeutic strategies', *Curr Pharm Des*, 9: 2385-402.
- Tejero, J., S. Shiva, and M. T. Gladwin. 2019. 'Sources of Vascular Nitric Oxide and Reactive Oxygen Species and Their Regulation', *Physiol Rev*, 99: 311-79.
- Tolle, M., A. Pawlak, M. Schuchardt, et al. 2008. 'HDL-associated lysosphingolipids inhibit NAD(P)H oxidase-dependent monocyte chemoattractant protein-1 production', *Arterioscler Thromb Vasc Biol*, 28: 1542-8.
- Touyz, R. M., X. Chen, F. Tabet, et al. 2002. 'Expression of a functionally active gp91phox-containing neutrophil-type NAD(P)H oxidase in smooth muscle cells from human resistance arteries: regulation by angiotensin II', *Circ Res*, 90: 1205-13.
- Touyz, R. M., A. C. Montezano, F. Rios, et al. 2017. 'Redox Stress Defines the Small Artery Vasculopathy of Hypertension: How Do We Bridge the Bench-to-Bedside Gap?', *Circ Res*, 120: 1721-23.
- Touyz, R. M., and E. L. Schiffrin. 2001. 'Increased generation of superoxide by angiotensin II in smooth muscle cells from resistance arteries of hypertensive patients: role of phospholipase D-dependent NAD(P)H oxidase-sensitive pathways', *J Hypertens*, 19: 1245-54.
- Vasan, R. S., J. C. Evans, M. G. Larson, et al. 2004. 'Serum aldosterone and the incidence of hypertension in nonhypertensive persons', *N Engl J Med*, 351: 33-41.
- Vaziri, N. D., K. Liang, and Y. Ding. 1999. 'Increased nitric oxide inactivation by reactive oxygen species in lead-induced hypertension', *Kidney Int*, 56: 1492-8.
- Versari, D., E. Daghini, A. Viridis, et al. 2009. 'Endothelial dysfunction as a target for prevention of cardiovascular disease', *Diabetes Care*, 32 Suppl 2: S314-21.
- Violi, F., P. Pignatelli, C. Pignata, et al. 2013. 'Reduced atherosclerotic burden in subjects with genetically determined low oxidative stress', *Arterioscler Thromb Vasc Biol*, 33: 406-12.
- Wallace, C., S. J. Newhouse, P. Braund, et al. 2008. 'Genome-wide association study identifies genes for biomarkers of cardiovascular disease: serum urate and dyslipidemia', *Am J Hum Genet*, 82: 139-49.
- Wang, A. Z., L. Li, B. Zhang, et al. 2011. 'Association of SNP rs17465637 on chromosome 1q41 and rs599839 on 1p13.3 with myocardial infarction in an American caucasian population', *Ann Hum Genet*, 75: 475-82.
- Warren, H. R., E. Evangelou, C. P. Cabrera, et al. 2017. 'Genome-wide association analysis identifies novel blood pressure loci and offers biological insights into cardiovascular risk', *Nat Genet*, 49: 403-15.
- Weber, M. A., E. L. Schiffrin, W. B. White, et al. 2014. 'Clinical practice guidelines for the management of hypertension in the community a statement by the American Society of Hypertension and the International Society of Hypertension', *J Hypertens*, 32: 3-15.
- White, C. N., G. A. Figtree, C. C. Liu, et al. 2009. 'Angiotensin II inhibits the Na⁺-K⁺ pump via PKC-dependent activation of NADPH oxidase', *Am J Physiol Cell Physiol*, 296: C693-700.
- Williams, B., G. Mancia, W. Spiering, et al. 2018. '2018 ESC/ESH Guidelines for the management of arterial hypertension', *Eur Heart J*, 39: 3021-104.
- Xiong, Y., P. Yang, R. L. Proia, et al. 2014. 'Erythrocyte-derived sphingosine 1-phosphate is essential for vascular development', *J Clin Invest*, 124: 4823-8.

- Yao, L., A. R. Folsom, J. S. Pankow, et al. 2016. 'Parathyroid hormone and the risk of incident hypertension: the Atherosclerosis Risk in Communities study', *J Hypertens*, 34: 196-203.
- Yoon, C. M., B. S. Hong, H. G. Moon, et al. 2008. 'Sphingosine-1-phosphate promotes lymphangiogenesis by stimulating S1P1/Gi/PLC/Ca²⁺ signaling pathways', *Blood*, 112: 1129-38.
- Yuan, Q., J. Yang, G. Santulli, et al. 2016. 'Maintenance of normal blood pressure is dependent on IP3R1-mediated regulation of eNOS', *Proc Natl Acad Sci U S A*, 113: 8532-7.
- Zeller, T., S. Blankenberg, and P. Diemert. 2012. 'Genomewide association studies in cardiovascular disease--an update 2011', *Clin Chem*, 58: 92-103.
- Zhang, Y., P. Murugesan, K. Huang, et al. 2020. 'NADPH oxidases and oxidase crosstalk in cardiovascular diseases: novel therapeutic targets', *Nat Rev Cardiol*, 17: 170-94.

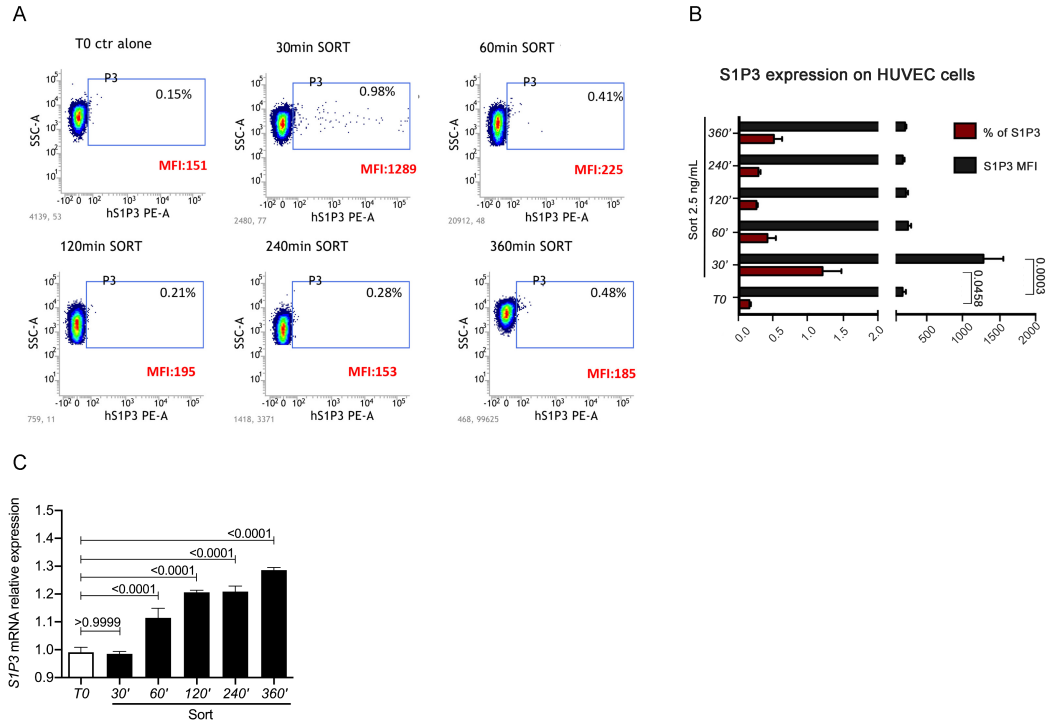
8. SUPPLEMENTARY FIGURES AND TABLES



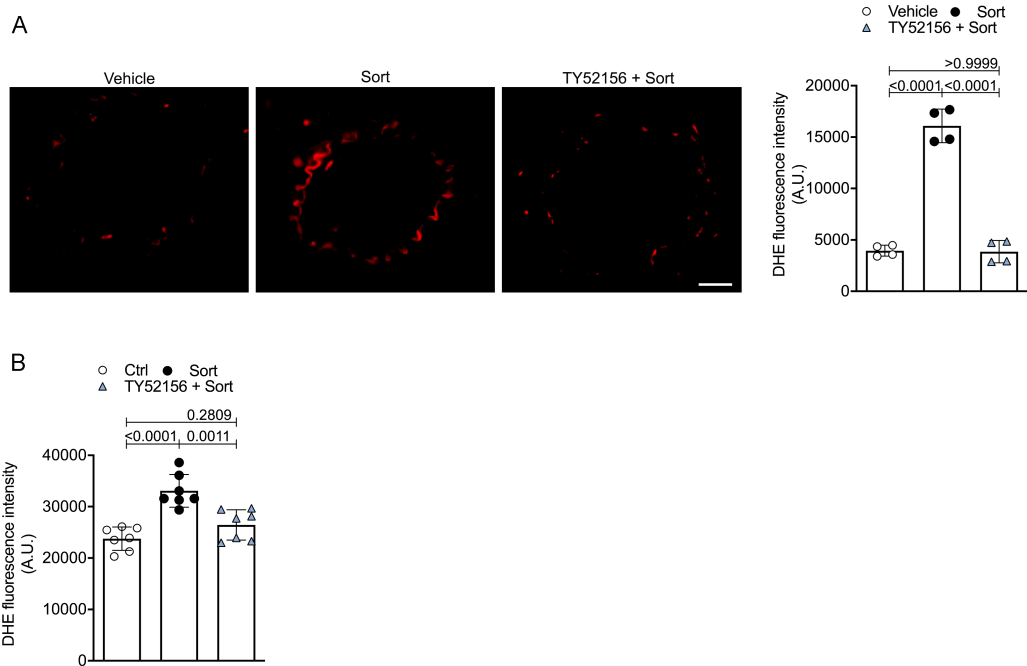
Supplemental Figure 1 Sortilin does not affect endothelial-independent vasorelaxation and vasoconstriction. (A) Acetylcholine (ACh)-evoked vasorelaxation in WT mice mesenteric arteries exposed to vehicle or sortilin (sort) at 1.25 ng/mL or to (B) 5 ng/mL for different preincubation times (30, 60, 120, 240, and 360 minutes); ($n=3-6$). Concentration-response curves to (C) nitroglycerin ($n=3-4$) and (D) to thromboxane mimetic U46619 ($n=6$) in WT mesenteric arteries treated with vehicle or 2.5 ng/mL of sortilin at different incubation times. Results are expressed as mean \pm SD. (B) * $P<0.0001$ vs. Basal at the same ACh concentration (as indicated by color code).



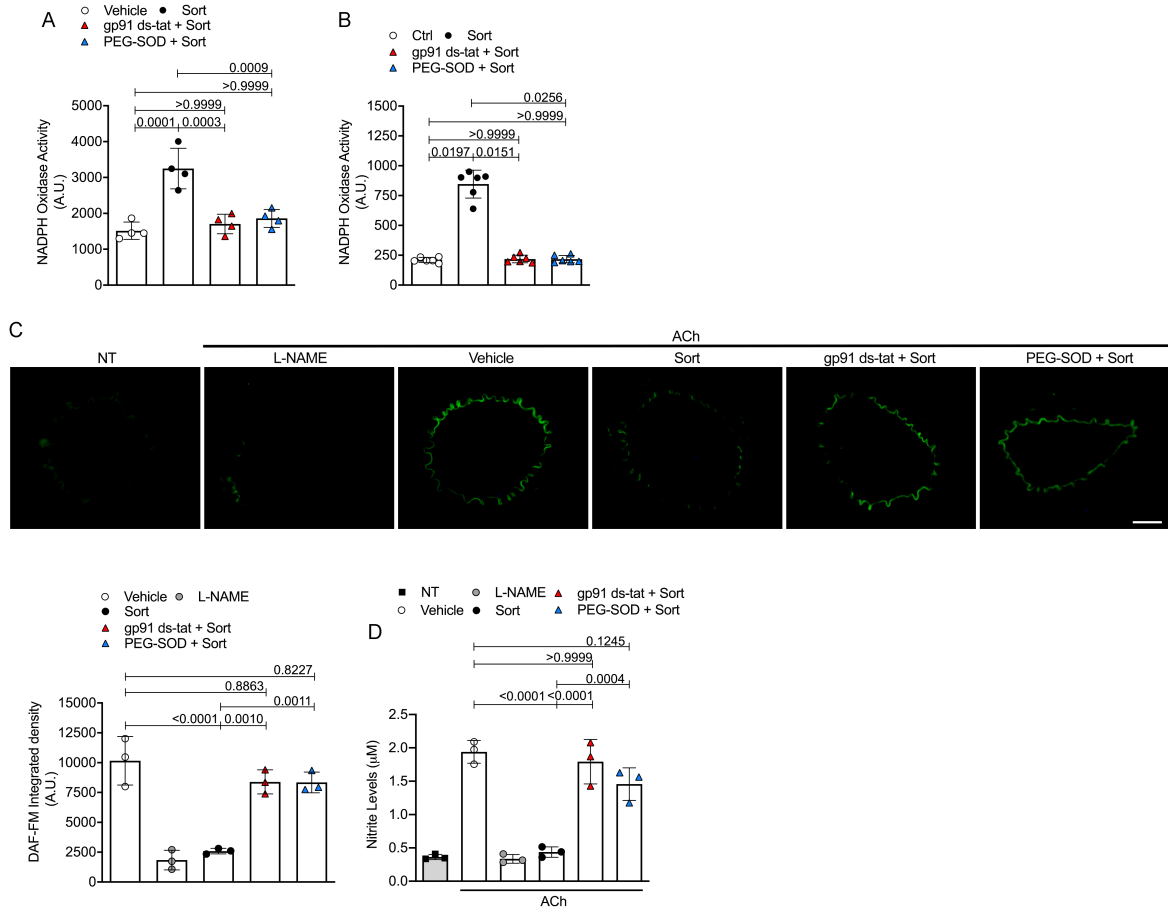
Supplemental Figure 2 Sortilin induces endothelial dysfunction by altering sphingolipid metabolism. (A) ACh-evoked vasorelaxation in WT mesenteric arteries exposed to vehicle or pretransfected with either siRNA targeting aCDase or a scrambled siRNA (si-SCR) and then exposed to vehicle or sortilin for 60 minutes. The effectiveness of silencing was determined by western blotting; (n=5). (B and C) ACh-evoked vasorelaxation in WT mesenteric arteries exposed to vehicle or pretransfected with either SphK1 siRNA, SphK2 siRNA or a scrambled siRNA (si-SCR) prior to 1 h treatment with vehicle or sortilin. The effectiveness of silencing was determined by Western blotting; (n=4-5). (D) Individual sphingolipid species measured by LC-MS/MS in HUVECs treated with vehicle (ctrl) or sortilin for 1 hr; (n=7). (E and F) ACh-evoked vasorelaxation in WT mesenteric arteries exposed to vehicle or pretransfected with either siRNA targeting aCDase or si-SCR and then exposed to (E) C16 or (F) C18 prior to vehicle or sortilin for 60 minutes; (n=3). Results are expressed as mean \pm SD. (C) * $P < 0.0001$ vs. Vehicle or Si-SCR + Vehicle at the same ACh concentration (as indicated by color code). (E) * $P < 0.005$ vs. Vehicle; # $p < 0.05$ vs. Vehicle, Si-SCR + C16 + Vehicle and Si-aCDase + C16 + Sort; ° $p < 0.005$ vs. Vehicle, Si-SCR + C16 + Vehicle and Si-aCDase + C16 + Sort at the same ACh concentration (as indicated by color code). (F) * $P < 0.05$ vs. Vehicle; # $p < 0.05$ vs. Vehicle, Si-SCR + C18 + Vehicle and Si-aCDase + C18 + Sort at the same ACh concentration (as indicated by color code).



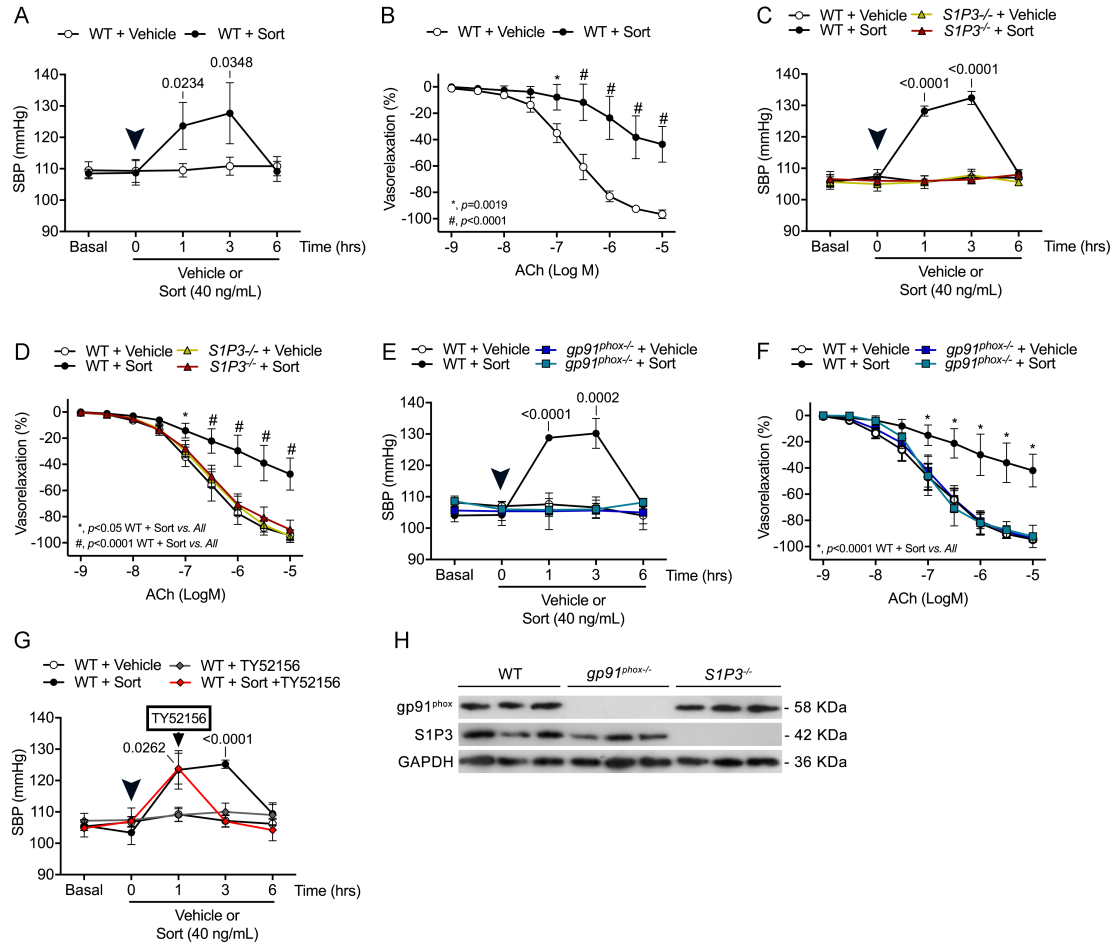
Supplemental Figure 3 S1P3 expression at different time points following sortilin stimulation in HUVEC cells. (A) Representative flow cytometry SSC vs S1P3 density plots for each experimental condition is presented. (B) Bars graph report both the percentage (red) of S1P3+ and mean fluorescence intensity (MFI) (black) of S1P3 receptor on viable HUVEC gated cells from 3 independent experiments. (C) mRNA expression of S1P3 determined by quantitative reverse transcription polymerase chain reaction in HUVECs treated at different timepoints with 2.5 ng/mL of sortilin; (n=3). Results are expressed as mean \pm SD.



Supplemental Figure 4 TY52156 prevents sortilin-induced ROS overproduction. (A) Representative images of Dihydroethidium (DHE, 2 $\mu\text{mol/L}$) staining of WT mesenteric arteries treated with vehicle, sortilin alone, or pretreated with the S1P3 inhibitor TY52156. Scale bar: 25 μm . Bar graph shows DHE fluorescence intensity; ($n=4$). (B) DHE fluorescence measurement by microplate reader in HUVECs treated with vehicle, sortilin alone, or pretreated with the S1P3 inhibitor TY52156; ($n=7$). Results are expressed as mean \pm SD.



Supplemental Figure 5 NOX2 inhibition protects from oxidative stress and NO impairment induced by sortilin. (A and B) Effect of sortilin on NADPH oxidase activity in (A) WT mice mesenteric arteries and in (B) HUVECs in presence of gp91 ds-tat or PEG-SOD; ($n=4$; $n=6$, respectively). (C) Detection of NO by DAF-FM fluorescence in untreated WT mesenteric arteries (NT), stimulated with ACh alone (10^{-5} M) (vehicle) or in presence of L-NAME, sortilin alone or pretreated with either gp91 ds-tat or PEG-SOD prior to sortilin. Scale bar: 25 μ m; bar graph gives mean of fluorescence integrated density of DAF-FM; ($n=3$). (D) NO metabolites concentration in supernatants of untreated mesenteric arteries (NT), stimulated with ACh alone (10^{-5} M) (vehicle) or in presence of L-NAME, sortilin alone or pretreated with either gp91 ds-tat or PEG-SOD prior to sortilin; ($n=3$). Results are expressed as mean \pm SD.



Supplemental Figure 6 Deletion of either *S1P3* or *gp91phox* protects from hypertension and endothelial dysfunction induced by acute sortilin administration. (A-F) WT, *S1P3*^{-/-}, and *gp91phox*^{-/-} mice analyzed for (A, C and E) systolic blood pressure (SBP) before and after an intraperitoneal (i.p.) bolus dose of sortilin (40ng/mL); (n=5-6), and (B, D and F) for ACh-induced endothelium-dependent vasodilation in mesenteric arteries 6 hours after sortilin injection; (n=3-4 WT, n=5 *S1P3*^{-/-}, n=4 *gp91phox*^{-/-}). (G) Time course of SBP measured in WT mice before and after (arrowheads) a single dose of sortilin (40 ng/mL, i.p.). 2 hours after sortilin injection, mice were administered TY52156 (i.p.), and their blood pressure measured 2 and 4 hours later; (n=5). (H) Western Blot analysis conducted on extracts of mesenteric arteries obtained from wild-type (WT), *gp91phox* or *S1P3* knockout mice. Data are expressed as mean \pm SD.

Table 1. Clinical characteristics of normotensive and hypertensive individuals from the Campania Salute Network Study.

Parameter	Normotensives (N=71)	Hypertensives (N=71)	P-Value
<i>Clinical characteristics</i>			
Age, years	64.1±7.6	63±8	0.388
Sex, M/F	36/35	37/34	>0.9999
SBP (mmHg)	119.1±3.1	142.3±14.8	<0.0001
DBP (mmHg)	78.3±3.1	88.4±9.5	<0.0001
TC (mg/dL)	176.5±29.2	183.7±21.7	0.24
HDL (mg/dL)	54±10.5	54.4±9.2	0.579
TG (mg/dL)	120.5±20.2	113.9±30.1	0.071
Glucose (mg/dL)	89.8±6	92.4±9.1	0.139
Creatinine (mg/dL)	0.86±0.08	0.89±0.2	0.121
<i>Medication, n (%)</i>			
β-blockers	0	16 (22.5)	
ARBs	0	29 (40.8)	
ACE-inhibitors	0	16 (22.5)	
Diuretics	0	25 (35.2)	
CCBs	0	22 (31)	

SBP, systolic blood pressure; DBP, diastolic blood pressure; TC, total cholesterol; HDL, high density lipoprotein; TG, triglycerides; ARBs, Angiotensin II receptor blockers; CCBs, Calcium channel blockers; VKAs, Vitamin K antagonists. *P*-value based on unpaired Student's *t*-test for continuous variables and Fisher's exact test for categorical variables.

Table 2. Clinical characteristics of individuals from the Moli-Sani Study.

Parameter	Hypertensives		Normotensives (N=89)	P-Value
	Controlled (N=91)	Uncontrolled (N=90)		
<i>Clinical characteristics</i>				
Age, years	61.4 ± 9.7	60.1 ± 9.8	60.2±9.3	0.56
Sex, M/F	43/48	40/50	43/46	0.865
SBP (mmHg)	129.9 ± 7.7 ^a	167.6 ± 17.6 ^{a,b}	121.9 ± 5.8	<0.001
DBP (mmHg)	78.1 ± 6.3 ^c	96.2 ± 6.2 ^{a,b}	73.6±5.4	<0.001
TC (mg/dL)	218.3 ± 37.4	221.9 ± 36.1	221.3 ± 39.5	0.65
HDL (mg/dL)	56.7 ± 13.7	57.3 ± 13.3	61.3 ± 17.6	0.17
TG (mg/dL)	122.7 ± 55.0	128.8 ± 53.8	119.2 ± 65.9	0.07
Glucose (mg/dL)	97.2 ± 10.9	97.7 ± 11.1	94.8 ± 11.4	0.13
Creatinine (mg/dL)	0.8 ± 0.2	0.9 ± 0.3	0.8 ± 0.1	0.11
WBC (10 ³ /μL)	6.0 ± 1.4	6.2 ± 1.4	6.0 ± 2.2	0.15
RBC (10 ³ /μL)	4.9 ± 0.4	5.0 ± 0.5	4.8 ± 0.7	0.11
Hgb (g/dL)	14.5 ± 1.3	14.7 ± 1.5	14.4 ± 1.3	0.48
Htc (%)	43.1 ± 3.6	43.6 ± 3.9	42.9 ± 3.8	0.67
MCV (fl)	88.8 ± 5.2	88.0 ± 6.0	89.8 ± 6.7	0.07
MCH (pg)	29.8 ± 2.1	29.7 ± 2.5	30.1 ± 2.6	0.39
MCHC (g/dl)	33.6 ± 1.1	33.7 ± 1.1	33.5 ± 1.1	0.40
RDW (%)	12.8 ± 0.7	13.0 ± 1.4	12.8 ± 0.9	0.72
PLT (10 ³ /μL)	251.2 ± 62.6	257.9 ± 62.7	251.1 ± 61.1	0.80
<i>Medication (%)</i>				
β-blockers	18 (20)	22 (20)	0	
ARBs	44 (48.8)	35 (38.4)	0	
ACE-inhibitors	26 (28.8)	36 (39.5)	0	
Diuretics	40 (44.4)	35 (38.4)	0	
CCBs	11 (12.2)	15 (16.4)	0	

SBP, systolic blood pressure; DBP, diastolic blood pressure; TC, total cholesterol; HDL, high density lipoprotein; TG, triglycerides; WBC, with blood cells; RBC, red blood cells; Hgb, hemoglobin; Htc, Hematocrit; MCV, mean cell volume; MCH, mean corpuscular hemoglobin; MCHC, mean corpuscular hemoglobin concentration; RDW, red cell distribution width; PLT, platelets; ARBs, Angiotensin II receptor blockers; CCBs, Calcium channel blockers. a, $p<0.001$ vs. normotensives; b, $p<0.001$ vs. controlled hypertensives; c, $p=0.008$ vs. normotensives.